

The 2-Dimensional Dual of ϕ^4 in AdS_3

Weichen Xiao , Ivo Sachs

*Arnold-Sommerfeld-Center for Theoretical Physics, Ludwig-Maximilians-Universität München,
Theresienstr. 37, 80333 Munich, Germany*

E-mail: w.xiao@lmu.de

ABSTRACT: We study the correlation functions of a conformally coupled ϕ^4 -interacting theory in AdS_3 and its dual CFT_2 . The one-loop diagram is not expressible in terms of known transcendental functions, but is shown to be expressible as an infinite sum of previously well-studied tree-level diagrams, and we compute this sum using several number-theoretic conjectures. This enables us to extract recursively, the analytic expressions of anomalous dimensions of all dual double-trace operators. In the s -channel various consistency checks were performed against established bootstrap method, while our results in the t - and u -channel are not available in any previous literature to our knowledge.

Contents

1	Introduction	1
2	Preliminaries	3
3	Cross Diagram	6
4	Loop diagrams	7
4.1	Fish diagram and tricks with conformal transformation	8
4.2	The s -channel as a cross check	10
5	Conformal block expansion in the t- and u-channel	13
5.1	Spectral function does not work easily for t and u channel	14
5.2	Conformal Block Expansion	15
5.3	The s channel as a warm-up	16
5.4	t - and u - channel anomalous dimensions	18
6	Conclusion	21
A	Loop calculation	22
B	Spectral Function	24
B.1	Disconnected Diagrams	25
B.2	Tree Level Contact interaction	25
B.3	One Loop Level	27
C	Conformal Block	28
D	Recursive Relation	30

1 Introduction

Anti-de Sitter space (AdS) and de Sitter space (dS) are two of the simplest spaces with non-vanishing curvature. Furthermore, the isometry group of AdS_{d+1} is isomorphic to the conformal group acting on its d -dimensional boundary. Consequently, any bulk theory with correlators invariant under AdS isometries are automatically conformal invariant, when the positions of operator insertions are taken the boundary limit. No conjectural input is required in this construction, as one is simply considering a restriction of the same underlying theory [1]. Given such bulk correlators, it is then possible to extract certain data of the dual CFT, namely the operator spectrum and OPE coefficients [2]. Within

this framework, numerous studies have been carried out for $\text{AdS}_{d+1}/\text{CFT}_d$ for a variety of dimensions.

As a concrete illustration of this idea, we consider a conformally coupled ϕ^4 interacting scalar field in the bulk of AdS_3 and attempt to extract its dual conformal data corresponding to loop corrections. Bulk loops in Anti-de Sitter space have been considered for some time [3–7]. In [3, 4], bulk one-loop diagrams for a conformally coupled scalar field with conformal dimensions $\Delta_- = 1$ and $\Delta_+ = 2$ were computed and these one-loop amplitudes were subsequently expanded in conformal cross ratios, enabling the extraction of anomalous dimensions in the dual perturbative CFT. A closed-form expression for these anomalous dimensions was obtained in [8]. In addition, the same concept was extended to the dS_4/CFT_3 correspondence in [9]. It is discovered in [10–13] that the cosmological in-in correlators in de Sitter space manifest as Witten diagrams involving a mixture of propagators with conformal dimension Δ_\pm . As a result, such correlators may be computed using the techniques developed in the aforementioned works, providing an alternative to the Schwinger-Keldysh formalism. This observation has motivated further studies of cosmological correlators, including [14, 15].

In this work, we focus on $\text{AdS}_3/\text{CFT}_2$ and study the four-point one-loop diagrams of a conformally coupled scalar field with conformal dimension $\Delta = \frac{3}{2}$. The three-dimensional bulk provides an interesting setting to investigate due to a balance of subtle complexity and simplicity. On one hand, the half-integer conformal dimension leads to non-integer powers in the Feynman integrals, rendering the corresponding computations effectively one loop order more involved than their counterparts in AdS_4 . As a consequence, we are unable to perform the conformal block expansion following the same approach as [3, 4]. Instead, we demonstrate a method in which loop-level amplitudes are expanded as a series of tree-level diagrams with increasing conformal weights on their external legs, whose conformal block expansions have been studied extensively in [16]. With the aid of two mathematical conjectures, we are able to resum this series and recover the exact values of anomalous dimensions in the dual CFT.

On the other hand, the three-dimensional bulk has the advantage that the ϕ^4 theory is finite in both the ultraviolet and infrared. This makes it a useful reference framework for developing intuition about regularization and renormalization in more general settings. In the s -channel, this simplicity enables an alternative bootstrap approach to extracting the same dual CFT data [5], resulting in a consistency check between direct bulk perturbative computations and the bootstrap of the spectral function, which we will verify explicitly in this paper. In contrast, the bootstrap method fails in the t - and u -channels due to the presence of nontrivial spin exchange in the double-trace operators. To the best of our knowledge, the t - and u -channel anomalous dimensions presented here are therefore the first results of their kind.

Last but not the least, $\text{AdS}_3/\text{CFT}_2$ correspondence builds a connection between quantum field theory in curved spacetime and two-dimensional conformal field theory, which is by far the best understood CFT among all dimensions. Our study in scalar field with $\Delta = \frac{3}{2}$ sheds light on the other possible conformally coupled scaling dimension, namely $\Delta = \frac{1}{2}$, which we believe might be connected to the two dimensional Ising model.

The main result of the paper are anomalous dimensions $\gamma_{n,l}$ that deforms the double trace operators $\mathcal{O}\square^n\partial^l\mathcal{O}$, as a result of s -, t - and u -channel one loop corrections in the bulk. A recursive relation has been found governing all anomalous dimensions as a function of n and l , which due to its lengthiness we present in Appendix D. Given the initial values, this recursive relation enables us to extract $\gamma_{n,l}$ at any given order of n and l efficiently. In addition, for $n = 0$ we found a closed form expression

$$\gamma_{0,l}^{s+t+u} = -\frac{\lambda^2}{32\pi^2(l+1)(2l+1)(2l+3)} - \frac{\lambda^2}{256\pi^2}\delta^{l0}. \quad (1.1)$$

The paper will be structured as follows: in Chapter 2 we introduce the preliminaries of a conformally coupled ϕ^4 theory in AdS_3 and its dual. In Chapter 3 we compute the tree level 'cross' diagram which not only contributes to the leading order anomalous dimensions and OPE coefficients, but also serves as building block for the one loop diagram. In Chapter 4 we demonstrate the trick of expressing the one loop diagram as an infinite sum of cross diagrams. As a consequence, in the s -channel the spectral function of the loop diagram can be read off directly as a corresponding sum. We then perform a consistency check by comparing this result with the spectral function obtained via bootstrap methods in [5]. In Chapter 5 we show that the same technique does not extend to the t - and u -channel. Instead, we carry out a conformal block expansion for each individual cross diagram appearing in the series. Subsequently, a resummation of the series expansion is performed using two conjectures proposed in this work, enabling us to guess a recursive relation governing the exact values of the anomalous dimensions.

2 Preliminaries

The $d+1$ dimensional (Euclidean)anti-de Sitter space ((E)AdS $_{d+1}$) is defined by an embedding in a $d+2$ dimensional Lorentzian space with metric

$$\eta_{\text{Euc}} = \text{diag}(1, \underbrace{-1, \dots, -1}_{d+1 \text{ times}}), \quad (2.1)$$

which is considered a fixed background, as in this paper we do not take into account any back reaction. The embedding takes the form

$$X^2 = X_0^2 - \sum_i X_i^2 = a^2. \quad (2.2)$$

We will work on the Poincaré patch of anti-de Sitter space, parameterized by

$$\begin{aligned} X_0 &= \frac{1}{2} \frac{z^2 + \vec{x}^2 + a^2}{z} \\ X_{d+1} &= \frac{1}{2} \frac{z^2 + \vec{x}^2 - a^2}{z} \\ X_i &= \frac{a}{z} x_i, \end{aligned} \quad (2.3)$$

so that η_{Euc} induces a hyperbolic metric

$$g_{\text{AdS}} = -\frac{1}{z^2}(dx_i^2 + dz^2). \quad (2.4)$$

We study a simple model of ϕ^4 interacting scalar field in AdS_3 , governed by the following action

$$S = \int_{\text{AdS}_3} d^3x \sqrt{|g_{\text{AdS}}|} \left(\frac{1}{2}(\partial\phi)^2 + \frac{1}{2}m^2\phi^2 + \xi R\phi^2 + \frac{\lambda}{4!}\phi^4 \right). \quad (2.5)$$

Furthermore, we assume the scalar field to be conformally coupled, so that the mass term cancels with the curvature term for $\xi = \frac{d-1}{4d}$, leaving the Lagrangian analogous to massless scalar theory in flat space. Hence it is required that

$$m^2 = -\frac{d^2 - 1}{4}a^2. \quad (2.6)$$

Since the AdS background is fixed, any theory in such background has to be invariant under the isometry group of AdS. On the other hand, an isometry group in AdS_{d+1} is isomorphic to a conformal group on the boundary CFT_d . Therefore the bulk theory automatically becomes a conformal field theory when the boundary limit is taken. A massive scalar field in the bulk is dual to an operator on the boundary with conformal dimension [17]

$$\Delta = \frac{d}{2} \pm \sqrt{\frac{d^2}{4} + \frac{m^2}{a^2}}. \quad (2.7)$$

For concreteness we will consider the + sign in this work. The minus sign does also have an interesting CFT dual that we will consider in a forthcoming work. Combining it with (2.6) yields

$$\Delta = \frac{3}{2}. \quad (2.8)$$

The bulk to bulk propagator of such a scalar field then takes the form (e.g. [2])

$$\begin{aligned} \Lambda(x, y, \Delta = \frac{3}{2}) &= \frac{a\sqrt{K_{xy}}}{4\sqrt{2}\pi} \left(\frac{1}{\sqrt{1 - K_{xy}}} - \frac{1}{\sqrt{1 + K_{xy}}} \right) \\ &= \frac{a}{4\sqrt{2}\pi} \left(\sqrt{\frac{2zw}{(x^i - y^i)^2 + (z - w)^2}} - \sqrt{\frac{2zw}{(x^i - y^i)^2 + (z + w)^2}} \right), \end{aligned} \quad (2.9)$$

where K_{xy} is an isometry invariant quantity defined by

$$K_{xy} = \frac{2zw}{(x^i - y^i)^2 + z^2 + w^2}, \quad (2.10)$$

that relates to the geodesic distance ρ_{xy} through $\frac{1}{K_{xy}} = \cosh a\rho_{xy}$. The presence of the square root in (2.9) presents a significant complication for the computation of Feynman integrals compared to even dimensional anti-de Sitter spaces where the propagator comes with integer powers for conformally coupled fields.

With the point (y, w) in (2.9) taken to the boundary, the bulk to boundary propagators reduces to

$$\begin{aligned}\bar{\Lambda}(x, y, \Delta) &= \frac{a}{4\sqrt{2\pi}} 2^{\frac{3}{2}-\Delta} w \bar{K}^\Delta \\ &= \frac{a}{2\pi} \left(\frac{wz}{(x-y)^2 + z^2} \right)^\Delta.\end{aligned}\quad (2.11)$$

Similarly, all positions of operator insertion in a four point function can be taken to the boundary, resulting in a conformal four point correlator [18, 19].

In conformal field theory, such correlator can be written as

$$\langle \mathcal{O}_\Delta(\vec{x}_1) \mathcal{O}_\Delta(\vec{x}_2) \mathcal{O}_\Delta(\vec{x}_3) \mathcal{O}_\Delta(\vec{x}_4) \rangle = \frac{N_\phi^2}{r_{12}^{2\Delta} r_{34}^{2\Delta}} \sum_{n=0, l=0, l \text{ even}}^{\infty} \mathcal{A}_{n,l} \mathcal{G}_{n,l}, \quad (2.12)$$

in which $\mathcal{G}_{n,l} = \mathcal{G}(\Delta(n, l), l)$ is the conformal block [20], defined in Appendix C, which forms a basis of conformal correlators. $\mathcal{A}_{n,l} = \mathcal{A}(\Delta(n, l), l)$ is the OPE coefficient squared, and N_ϕ is the normalization of bulk to boundary propagator that is factored out for consistency with [4] [8]. In our setting of $d = 2$ and $\Delta = \frac{3}{2}$, $N_\phi = \frac{a}{2\pi}$. Due to crossing symmetry the conformal block expansion can be equivalently done in the s , t , or u -channel. Here we choose the s -channel which corresponds to the OPE for small r_{12} and r_{34} .

For a free scalar field theory in AdS, its dual correlator is that of a generalized free field [1, 21] for which the composite, or double trace operators of the form $\mathcal{O}_\Delta \square^n \partial^l \mathcal{O}_\Delta$ carry conformal dimension

$$\Delta^{\text{free}}(n, l) = 2\Delta + 2n + l. \quad (2.13)$$

The four point correlator of a free theory then admits the following OPE

$$\begin{aligned}\langle \mathcal{O}_\Delta(\vec{x}_1) \mathcal{O}_\Delta(\vec{x}_2) \mathcal{O}_\Delta(\vec{x}_3) \mathcal{O}_\Delta(\vec{x}_4) \rangle_{\text{disc}} &= \sum_{n=0, l=0, l \text{ even}}^{\infty} \mathcal{A}(\Delta^{\text{free}}(n, l), l) \mathcal{G}(\Delta^{\text{free}}(n, l), l) \\ &:= \sum_{n=0, l=0, l \text{ even}}^{\infty} \mathcal{A}_{n,l} \mathcal{G}_{n,l}.\end{aligned}\quad (2.14)$$

The left hand side can be expressed as a disconnected AdS field theory 4-point function [4]:

$$\begin{aligned}\langle \mathcal{O}_\Delta(\vec{x}_1) \mathcal{O}_\Delta(\vec{x}_2) \mathcal{O}_\Delta(\vec{x}_3) \mathcal{O}_\Delta(\vec{x}_4) \rangle_{\text{disc}} &= \text{Diagram 1} + \text{Diagram 2} + \text{Diagram 3} \\ &= \Lambda(x_1, x_3) \Lambda(x_2, x_4) + \Lambda(x_1, x_2) \Lambda(x_3, x_4) + \Lambda(x_1, x_4) \Lambda(x_2, x_3) \\ &= \frac{N_\phi^2}{(r_{12} r_{34})^{2\Delta}} \left(1 + u^\Delta + \frac{u^\Delta}{v^\Delta} \right) \\ &= \frac{N_\phi^2}{(r_{12} r_{34})^{2\Delta}} \left(1 + u^\Delta \left(2 + \sum_{n=1}^{\infty} \frac{\Gamma(\Delta+n)}{\Gamma(\Delta)\Gamma(n+1)} \right) (1-v)^n \right),\end{aligned}\quad (2.15)$$

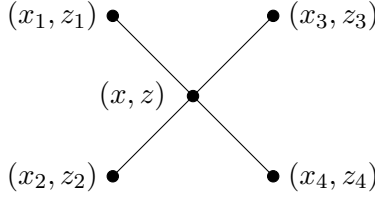


Figure 1. The cross diagram \mathcal{I}_4

where $r_{ij} = |\vec{x}_i - \vec{x}_j|$ and $N_\phi = \frac{a}{2\pi}$ originated from (2.11). The conformal cross ratios u and v are defined by

$$u = \frac{r_{12}^2 r_{34}^2}{r_{13}^2 r_{24}^2} \quad v = \frac{r_{14}^2 r_{23}^2}{r_{13}^2 r_{24}^2}. \quad (2.16)$$

At higher loop order, $\Delta(n, l)$ deviates from its generalized free field value, obtaining corrections of the form

$$\Delta_{(n,l)} \rightarrow \Delta_{(n,l)} + \sum_{p=0}^{\infty} \gamma_{n,l}^{(p)}(\Delta). \quad (2.17)$$

This results in $\mathcal{A}_{n,l}$ and $\mathcal{G}_{n,l}$ also being perturbatively corrected as follows,

$$\begin{aligned} \mathcal{A}_{n,l}(\Delta) &= A_{n,l}(\Delta) + (\gamma_{n,l}^{(1)}(\Delta) + \gamma_{n,l}^{(2)}(\Delta)) A_{n,l}^{(1)} + \frac{1}{2} (\gamma_{n,l}^{(1)}(\Delta))^2 A_{n,l}^{(2)} + \dots \\ \mathcal{G}_{n,l} &= G_{n,l} + (\gamma_{n,l}^{(1)}(\Delta) + \gamma_{n,l}^{(2)}(\Delta)) \underbrace{\frac{\partial G_{n,l}}{\partial \Delta} \Big|_{\Delta(n,l)}}_{G'_{n,l}} + \frac{1}{2} (\gamma_{n,l}^{(1)}(\Delta))^2 \underbrace{\frac{\partial^2 G_{n,l}}{\partial \Delta^2} \Big|_{\Delta(n,l)}}_{G''_{n,l}} + \dots, \end{aligned}$$

so that

$$\begin{aligned} \mathcal{A}_{n,l} \mathcal{G}_{n,l} &= A_{n,l} G_{n,l} + \gamma_{n,l}^{(1)}(\Delta) \left(A_{n,l} G'_{n,l} + A_{n,l}^{(1)} G_{n,l} \right) \\ &\quad + \frac{1}{2} (\gamma_{n,l}^{(1)}(\Delta))^2 \left(A_{n,l} G''_{n,l} + A_{n,l}^{(2)} G_{n,l} + 2 A_{n,l}^{(1)} G'_{n,l} \right) \\ &\quad + \gamma_{n,l}^{(2)}(\Delta) \left(A_{n,l} G'_{n,l} + A_{n,l}^{(1)} G_{n,l} \right) + \mathcal{O}(\lambda^3). \end{aligned} \quad (2.18)$$

The goal of this paper is then to extract $\gamma_{n,l}^{(1)}$, $\gamma_{n,l}^{(2)}$, $A_{n,l}^{(1)}$ and $A_{n,l}^{(2)}$, which characterizes the CFT that is dual to the bulk scalar field at each perturbative order.

3 Cross Diagram

To lowest order in the perturbation, the bulk correction is given by the four point function, the cross diagram \mathcal{I}_4 , as expressed in (3.1) and Figure 1.

$$\mathcal{I}_4 = \int d^{d+1}x \sqrt{|g_x|} \Lambda(x, x_1, \Delta_1) \Lambda(x, x_2, \Delta_2) \Lambda(x, x_3, \Delta_3) \Lambda(x, x_4, \Delta_4) \quad (3.1)$$

The method of calculating such integrals is already well-developed in previous works [22] and [20] for general dimensions. Here we do a quick recap of their first few steps in order to

fix our normalization relative to the references. Inserting the bulk to boundary propagator (2.11), the cross diagram then reads

$$\mathcal{I}_4 = \prod_{i=1}^4 z_i^{\Delta_i} \int d^{d+1}y \frac{a^{4-d-1}}{16\pi^4} z^{\Delta_1+\Delta_2+\Delta_3+\Delta_4-d-1} \prod_{i=1}^4 \left(\frac{1}{(x-x_i)^2 + z^2} \right)^{\Delta_i} \quad (3.2)$$

Making use of the Schwinger parametrization and defining $C = \frac{a^{4-d-1}}{16\pi^4} \prod_{i=1}^4 z_i^{\Delta_i}$, $\Lambda = \sum_i \lambda_i$ and $\mu = \frac{1}{2} \sum_{i=1}^4 \Delta_i$,

$$\begin{aligned} \mathcal{I}_4 = & C \int_0^\infty dz \frac{z^{2\mu-d-1}}{\prod_{i=1}^4 \Gamma(\Delta_i)} \int_0^\infty d\lambda_1 d\lambda_2 d\lambda_3 d\lambda_4 \\ & \prod_{i=1}^4 \lambda_i^{\Delta_i} \pi^{\frac{1}{2}d} \Lambda^{-\frac{1}{2}d} e^{-\frac{1}{\Lambda}(\sum_{i < j} \lambda_i \lambda_j r_{ij}^2)} e^{-\Lambda z^2}. \end{aligned} \quad (3.3)$$

Substituting $t = \Lambda z^2$,

$$\begin{aligned} \mathcal{I}_4 = & C \int_0^\infty dt d\lambda_1 d\lambda_2 d\lambda_3 d\lambda_4 \frac{t^{\mu-\frac{1}{2}d-1}}{2 \prod_{i=1}^4 \Gamma(\Delta_i) \Lambda^{\mu-\frac{1}{2}d}} \\ & \prod_{i=1}^4 \lambda_i^{\Delta_i} \pi^{\frac{1}{2}d} \Lambda^{-\frac{1}{2}d} e^{-\frac{1}{\Lambda}(\sum_{i < j} \lambda_i \lambda_j r_{ij}^2)} e^{-t}. \end{aligned} \quad (3.4)$$

By the definition of Gamma function, this is equivalent to

$$\begin{aligned} \mathcal{I}_4 = & C \frac{\pi^{\frac{1}{2}d} \Gamma(\mu - \frac{1}{2}d)}{2 \prod_{i=1}^4 \Gamma(\Delta_i)} \int_0^\infty d\lambda_1 d\lambda_2 d\lambda_3 d\lambda_4 \frac{1}{\Lambda^\mu} \\ & \prod_{i=1}^4 \lambda_i^{\Delta_i} e^{-\frac{1}{\Lambda}(\sum_{i < j} \lambda_i \lambda_j r_{ij}^2)}. \end{aligned} \quad (3.5)$$

Defining I_4 to be the same as in [22, B.5], we have the following normalization

$$\mathcal{I}_4 = \frac{\pi^{\frac{d}{2}}}{\prod_{i=1}^4 \Gamma(\Delta_i)} \left(\frac{a}{2\pi} \right)^4 \frac{\Gamma(\frac{\Delta_1+\Delta_2+\Delta_3+\Delta_4}{2} - \frac{d}{2})}{2} I_4 \quad (3.6)$$

and the explicit expression of I_4 is given by [22, B.11].

4 Loop diagrams

The main focus of this paper is to compute anomalous dimensions and OPE coefficients due to the 1-loop corrections to the four point correlator as shown in (4.1).

$$\begin{aligned} W^{\propto} = & \frac{\lambda^2}{2} (\mathcal{K}_4^s + \mathcal{K}_4^t + \mathcal{K}_4^u) \\ = & \frac{\lambda^2}{2} \left(\underbrace{\text{Diagram } s\text{-channel}}_{s\text{-channel}} + \underbrace{\text{Diagram } t\text{-channel}}_{t\text{-channel}} + \underbrace{\text{Diagram } u\text{-channel}}_{u\text{-channel}} \right), \end{aligned} \quad (4.1)$$

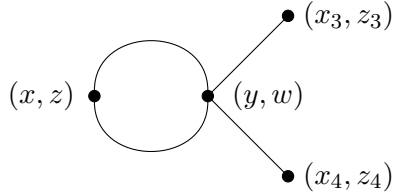


Figure 2. The fish diagram \mathcal{J}_4

in which the factor $\frac{1}{2}$ came from the symmetry factor of the one loop diagram. Unlike the cross diagram there is no general expression like (3.6) for this integral for generic dimensions and conformal weights. For the s -channel diagram it is convenient to use a spectral representation. In [5] the spectral function $\sigma(\nu)$ was then derived by a bootstrap approach resulting in a simple expression for $d < 3$ [5]. For $d = 3$, $\sigma(\nu)$ is divergent and requires renormalization [23].

For the t - and u -channel diagrams, the bootstrap of [5] does not apply. In principle, it is possible to extract the t -channel OPE form that of the s -channel (e.g. [24]). However, in practice we found this not computable. We will comment more on this in Section 5. Therefore, we will have to use a different approach in the following sections which we structure as follows: in Section 4.1. we discuss the fish diagram, as shown in Figure 2, which serves as a stepping stone for further computations of the full diagrams in all 3 channels. For the s - channel, we found two distinct methods to extract the dual CFT data: spectral function and conformal block expansion. The former method, demonstrated in Section 4.2, serves as a crosscheck with well established results in [5]. We leave the latter method to Section 5.3 where the consistency of the two methods will be shown in the s -channel. For the t - and u -channel, however, it is impossible to directly extract the spectral function and hence conformal block expansion is mandatory, which will be left to Section 5.4 as well.

4.1 Fish diagram and tricks with conformal transformation

To start with, we first consider the 'fish' diagram \mathcal{J}_4 (as shown in Figure 2) to which we will eventually attach the two remaining external legs as in [4]. It reads

$$\mathcal{J}_4 = \int d^3y \sqrt{|g_y|} \Lambda(x, y)^2 \bar{\Lambda}(y, x_3) \bar{\Lambda}(y, x_4). \quad (4.2)$$

Details of such loop integral are shown in Appendix A, giving the following result:

$$\mathcal{J}_4 = \frac{a\lambda}{128\pi^3} (z_3 z_4)^{\frac{3}{2}} (\bar{K}_{xx_3} \bar{K}_{xx_4})^{\frac{3}{2}} \left(\sqrt{1 + \alpha^2} \text{EllipticE}[-\alpha^2] - (1 + \alpha^2) \right), \quad (4.3)$$

where $\text{EllipticE}[x]$ is the complete elliptic integral of the second kind and the covariant quantity $\alpha = \frac{|x_3''|}{z''}$ is related to the geodesic distance through

$$\frac{4z''^2}{x_3''^2 + z''^2} = r_{34}^2 \bar{K}_{xx_3} \bar{K}_{xx_4} = \frac{4}{\alpha^2 + 1}. \quad (4.4)$$

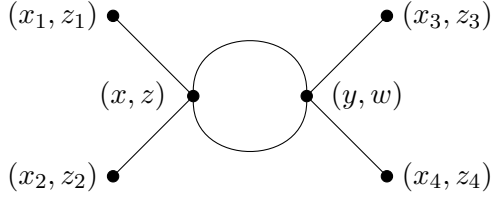


Figure 3. The full one-loop diagram \mathcal{K}_4

Proceeding as in $d = 3$ would require evaluating integrals similar to those appearing in [4, Appendix A], which we were unable to expand in terms of conformal invariants. Instead, a key observation of this paper is that the elliptic integral has a series expansion in $1 + \alpha^2$, such that

$$\begin{aligned}
\mathcal{J}_4 &= \frac{a\lambda}{128\pi^3} (z_3 z_4)^{\frac{3}{2}} (\bar{K}_{xx_3} \bar{K}_{xx_4})^{\frac{3}{2}} \sum_{k=0}^{\infty} \left(C_k (1 + \alpha^2)^{-k} + D_k (1 + \alpha^2)^{-k} \log(1 + \alpha^2) \right) \\
&= \frac{a\lambda}{128\pi^3} (z_3 z_4)^{\frac{3}{2}} (\bar{K}_{xx_3} \bar{K}_{xx_4})^{\frac{3}{2}} \sum_{k=0}^{\infty} \left(C_k (1 + \alpha^2)^{-k} - D_k \frac{d}{d\epsilon} \Big|_{\epsilon=0} (1 + \alpha^2)^{-k-\epsilon} \right) \\
&= \frac{a\lambda}{128\pi^3} (z_3 z_4)^{\frac{3}{2}} (\bar{K}_{xx_3} \bar{K}_{xx_4})^{\frac{3}{2}} \sum_{k=0}^{\infty} \left(C_k \left(\frac{r_{34}^2 \bar{K}_{xx_3} \bar{K}_{xx_4}}{4} \right)^k - D_k \frac{d}{d\epsilon} \Big|_{\epsilon=0} \left(\left(\frac{r_{34}^2 \bar{K}_{xx_3} \bar{K}_{xx_4}}{4} \right)^{k+\epsilon} \right) \right)
\end{aligned} \tag{4.5}$$

with series coefficients

$$C_k = -\frac{\left(\frac{1}{2}\right)_k \left(\frac{3}{2}\right)_k (1 + (2 + 6k + 4k^2)\psi(\frac{1}{2} + k) - (2 + 6k + 4k^2)\psi(1 + k))}{4(1 + 3k + 2k^2)k!(1 + k)!}, \tag{4.6}$$

and

$$D_k = \frac{\left(\frac{1}{2}\right)_k \left(\frac{3}{2}\right)_k}{4k!(1 + k)!}. \tag{4.7}$$

Then, recalling the bulk-to-boundary propagators from (2.11), eqn. (4.5) becomes

$$\begin{aligned}
\mathcal{J}_4 &= \frac{\lambda}{4\pi a} (z_3 z_4)^{\frac{3}{2}} \sum_{k=0}^{\infty} C_k (r_{34}^2)^k \bar{\Lambda}(x, x_3, \frac{3}{2} + k) \bar{\Lambda}(x, x_4, \frac{3}{2} + k) \\
&\quad - \frac{\lambda}{4\pi a} (z_3 z_4)^{\frac{3}{2}} \sum_{k=0}^{\infty} D_k \frac{d}{d\epsilon} \Big|_{\epsilon=0} (r_{34}^2)^{k+\epsilon} \bar{\Lambda}(x, x_3, \frac{3}{2} + k + \epsilon) \bar{\Lambda}(x, x_4, \frac{3}{2} + k + \epsilon),
\end{aligned} \tag{4.8}$$

where the factor of $(\frac{1}{4})^{\frac{3}{2}+k+\epsilon}$ in (4.5) contributes to the $2^{\frac{3}{2}-\Delta}$ factor in the propagator (2.11). Attaching the two missing legs we then find

$$\begin{aligned}
\mathcal{K}_4^s &= \int d^3x \frac{\lambda^2}{4\pi a} \sum_{k=0}^{\infty} C_k (r_{34}^2)^k \bar{\Lambda}(x, x_1, \frac{3}{2}) \bar{\Lambda}(x, x_2, \frac{3}{2}) \bar{\Lambda}(x, x_3, \frac{3}{2} + k) \bar{\Lambda}(x, x_4, \frac{3}{2} + k) \\
&\quad - \int d^3x \frac{\lambda^2}{4\pi a} \sum_{k=0}^{\infty} D_k \frac{d}{d\epsilon} \Big|_{\epsilon=0} (r_{34}^2)^{k+\epsilon} \bar{\Lambda}(x, x_1, \frac{3}{2}) \bar{\Lambda}(x, x_2, \frac{3}{2}) \bar{\Lambda}(x, x_3, \frac{3}{2} + k + \epsilon) \bar{\Lambda}(x, x_4, \frac{3}{2} + k + \epsilon) \\
&= \frac{\lambda^2}{4\pi a} \sum_{k=0}^{\infty} C_k (r_{34}^2)^k \mathcal{I}_4(\frac{3}{2}, \frac{3}{2}, \frac{3}{2} + k, \frac{3}{2} + k) \\
&\quad - \frac{\lambda^2}{4\pi a} \sum_{k=0}^{\infty} D_k \frac{d}{d\epsilon} \Big|_{\epsilon=0} (r_{34}^2)^{k+\epsilon} \mathcal{I}_4(\frac{3}{2}, \frac{3}{2}, \frac{3}{2} + k + \epsilon, \frac{3}{2} + k + \epsilon). \tag{4.9}
\end{aligned}$$

As shown diagrammatically in (4.10), we managed to rewrite a four point, one-loop diagram as a series of tree level diagrams, reducing the loop number by 1 at the cost of now having an infinite series to sum over.

$$\begin{array}{ccc}
\text{Diagram: } & & \\
\text{Diagram: } & = \sum_{k \geq 0} C_k & \text{Diagram: } + \sum_{k \geq 0} D_k \frac{d}{d\epsilon} \Big|_{\epsilon=0} \\
\text{Diagram: } & & \text{Diagram: }
\end{array} \tag{4.10}$$

This is the key equation which will allow us to extract contributions from the t - and u -channel bubble diagram to the conformal dimensions of the double trace operators in term of tree-level data.

In order to demonstrate that the series expansion trick preserves conformal covariance, below we make use of the representation of I_4 in [22],

$$\begin{aligned}
I_4(\delta_1, \delta_2, \delta_3, \delta_4) &= \frac{1}{r_{13}^{2\mu}} \left(\frac{r_{14}}{r_{24}} \right)^{2\delta_2} \left(\frac{r_{14}}{r_{34}} \right)^{2\delta_3-2\mu} \left(\frac{r_{13}}{r_{34}} \right)^{2\delta_4} \\
&\quad \times H(\delta_2, \mu - \delta_4, \delta_1 + \delta_2 + 1 - \mu, \delta_1 + \delta_2; u, v) \\
&= \frac{1}{r_{13}^{2\mu}} \left(\frac{r_{13}}{r_{23}} \right)^{2\delta_2} \left(\frac{r_{12}}{r_{23}} \right)^{2\delta_3-2\mu} \left(\frac{r_{12}}{r_{24}} \right)^{2\delta_4} \\
&\quad \times H(\delta_4, \mu - \delta_2, \delta_3 + \delta_4 + 1 - \mu, \delta_3 + \delta_4; u, v), \tag{4.11}
\end{aligned}$$

where $\mu = \frac{1}{2}(\delta_1 + \delta_2 + \delta_3 + \delta_4)$ and H is a conformal invariant quantity. For the s -channel we will use the first identity in (4.11) where the factor of $(r_{34}^2)^{k+\epsilon}$ in (4.9) is precisely canceled by $r_{13}^{-3} r_{24}^{-3} r_{34}^{-2k-2\epsilon}$ in front of H , leaving us with $r_{12}^{-3} r_{34}^{-3} u^{\frac{3}{2}}$ which exhibits the correct covariant behavior of a conformal correlator. For the t - and u -channel the second identity is to be used and a similar argument follows. The explicit expression of H is not immediately useful and we define them later in (5.10) and (5.11).

4.2 The s -channel as a cross check

From (4.9) we can already extract dual CFT data of the s -channel diagram by reading off the spectral function. Of course, its explicit expression for the s -channel has already been

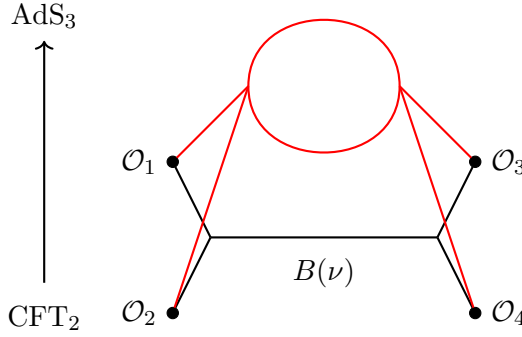


Figure 4. The intermediate double trace operator dual to a bubble diagram in the bulk

determined in [5] through a bootstrap. In this section we intend to perform a crosscheck between the bootstrapped spectral function and our results obtained from perturbative calculation. A recap on spectral functions of AdS correlators and their relationship to the dual CFT is recapped in Appendix B.

As in [23] we rewrite the four point correlation function in terms of a spectral representation

$$W(x_1, x_2, x_3, x_4) = \int_{\mathbb{R}} d\nu D(\nu) g_{x_1, x_2, x_3, x_4, \nu}^{\Delta, \Delta, \Delta, \Delta}, \quad (4.12)$$

where $D(\nu)$ is the 'spectral function'¹ and $g_{x_1, x_2, x_3, x_4, \nu}^{\Delta, \Delta, \Delta, \Delta}$ is the conformal block with an intermediate double trace operator of dimension $\Delta(\nu) = \frac{d}{2} + i\nu$. The latter is related to the conformal partial wave

$$\Psi_{x_1, x_2, x_3, x_4, \nu}^{\Delta, \Delta, \Delta, \Delta} = \int_{\partial \text{AdS}_{d+1}} d^d x \langle \mathcal{O}_\Delta(x_1) \mathcal{O}_\Delta(x_2) \mathcal{O}_{\frac{d}{2}+i\nu}(x_0) \rangle \langle \mathcal{O}_{\frac{d}{2}-i\nu}(x_0) \mathcal{O}_\Delta(x_3) \mathcal{O}_\Delta(x_4) \rangle \quad (4.13)$$

by a normalization, i.e.

$$\Psi_{x_1, x_2, x_3, x_4, \nu}^{\Delta, \Delta, \Delta, \Delta} = K(\nu) g_{x_1, x_2, x_3, x_4, \nu}^{\Delta, \Delta, \Delta, \Delta}, \quad (4.14)$$

$$K(\nu) = \frac{\pi^{\frac{d}{2}} \Gamma(-i\nu) \Gamma(\frac{d}{4} + i\frac{\nu}{2})^2}{\Gamma(\frac{d}{2} + i\nu) \Gamma(\frac{d}{4} - i\frac{\nu}{2})}. \quad (4.15)$$

In (4.13), explicit expression of the CFT 3-point function reads

$$\langle \mathcal{O}_\Delta(x_i) \mathcal{O}_\Delta(x_i) \mathcal{O}_{\frac{d}{2}+i\nu}(x_0) \rangle = \frac{1}{x_{ij}^{2\Delta-\Delta(\nu)} x_{i0}^{\Delta(\nu)} x_{j0}^{\Delta(\nu)}}. \quad (4.16)$$

which is related to the field theory correlator by a normalization $b_{\Delta, \Delta, \nu}$ defined in (B.4). Moreover, a reconstruction of the cross diagram in terms of the conformal partial wave is given in (B.6). Therefore, reconstructing each individual cross diagram appearing in the

¹As opposed to the actual Källén–Lehmann spectral representation of the two point function, $B(\nu)$, seen in (B.15)

sum (4.9) yields

$$\begin{aligned}
\mathcal{K}_4^s &= \frac{\lambda^2}{4\pi a} \sum_{k=0}^{\infty} C_k (r_{34}^2)^k \int_{\mathbb{R}} d\nu \frac{\nu^2}{\pi} b_{\Delta, \Delta, \nu} b_{\Delta+k, \Delta+k, -\nu} \Psi_{x_1, x_2, x_3, x_4, \nu}^{\Delta, \Delta, \Delta+k, \Delta+k} \\
&\quad - \frac{\lambda^2}{4\pi a} \sum_{k=0}^{\infty} D_k \frac{d}{d\epsilon} \Big|_{\epsilon=0} (r_{34}^2)^{k+\epsilon} \int_{\mathbb{R}} d\nu \frac{\nu^2}{\pi} b_{\Delta, \Delta, \nu} b_{\Delta+k+\epsilon, \Delta+k+\epsilon, -\nu} \Psi_{x_1, x_2, x_3, x_4, \nu}^{\Delta, \Delta, \Delta+k+\epsilon, \Delta+k+\epsilon} \\
&= \frac{\lambda^2}{4\pi a} \sum_{k=0}^{\infty} C_k \int_{\mathbb{R}} d\nu \frac{\nu^2}{\pi} b_{\Delta, \Delta, \nu} b_{\Delta+k, \Delta+k, -\nu} \Psi_{x_1, x_2, x_3, x_4, \nu}^{\Delta, \Delta, \Delta, \Delta} \\
&\quad - \frac{\lambda^2}{4\pi a} \sum_{k=0}^{\infty} D_k \frac{d}{d\epsilon} \Big|_{\epsilon=0} \int_{\mathbb{R}} d\nu \frac{\nu^2}{\pi} b_{\Delta, \Delta, \nu} b_{\Delta+k+\epsilon, \Delta+k+\epsilon, -\nu} \Psi_{x_1, x_2, x_3, x_4, \nu}^{\Delta, \Delta, \Delta, \Delta},
\end{aligned} \tag{4.17}$$

where in the last step we used the following relation between conformal partial waves:

$$\begin{aligned}
&\Psi_{x_1, x_2, x_3, x_4, \nu}^{\Delta, \Delta, \Delta+k+\epsilon, \Delta+k+\epsilon} \\
&= \int_{\partial \text{AdS}_{d+1}} d^d x_0 \langle \mathcal{O}_\Delta(x_1) \mathcal{O}_\Delta(x_2) \mathcal{O}_{\frac{d}{2}+i\nu}(x_0) \rangle \langle \mathcal{O}_{\frac{d}{2}-i\nu}(x_0) \mathcal{O}_{\Delta+k+\epsilon}(x_3) \mathcal{O}_{\Delta+k+\epsilon}(x_4) \rangle \\
&= \int_{\partial \text{AdS}_{d+1}} d^d x_0 \frac{1}{x_{12}^{2\Delta-\Delta(\nu)} x_{10}^{\Delta(\nu)} x_{20}^{\Delta(\nu)}} \frac{1}{x_{34}^{2\Delta+2k+2\epsilon-\Delta(\nu)} x_{30}^{\Delta(\nu)} x_{40}^{\Delta(\nu)}} \\
&= \frac{1}{(r_{34}^2)^{k+\epsilon}} \Psi_{x_1, x_2, x_3, x_4, \nu}^{\Delta, \Delta, \Delta, \Delta}.
\end{aligned} \tag{4.18}$$

It is then easy to read off

$$\begin{aligned}
B^{\text{perturb}}(\nu) &= \frac{1}{2} \frac{\lambda}{4\pi a} \sum_{k=0}^{\infty} \left(C_k (r_{34}^2)^k \frac{b_{\Delta+k, \Delta+k, -\nu}}{b_{\Delta, \Delta, \nu}} - D_k \frac{d}{d\epsilon} \Big|_{\epsilon=0} (r_{34}^2)^{k+\epsilon} \frac{b_{\Delta+k+\epsilon, \Delta+k+\epsilon, -\nu}}{b_{\Delta, \Delta, \nu}} \right) \\
&:= \sum_{k=0}^{\infty} B^k(\nu),
\end{aligned} \tag{4.19}$$

where the $\frac{1}{2}$ came from the symmetry factor of the one loop diagram.

On the other hand, through bootstrap it was found in [5] that for $d=2$,

$$B^{\text{bootstrap}}(\nu) = \frac{\lambda i}{2} \frac{(\Psi(\Delta - \frac{1+i\nu}{2}) - \Psi(\Delta - \frac{1-i\nu}{2}))}{8\pi\nu} \tag{4.20}$$

in which Ψ is the digamma function. Our next goal is to show that (4.19) and (4.20) are equivalent and give the same CFT data on the boundary.

In Appendix B, we derived the following expression of anomalous dimension and OPE coefficient depending on the spectral functions,

$$\gamma_{n,0}^{(2)} = \gamma_{n,0}^{(1)} B_{\nu_n}^{(0)}, \tag{4.21}$$

and

$$A_{n,0}^{(2)} = \frac{2\pi i}{(\gamma_{n,0}^{(1)})^2} (D_{\nu_n}^{\times(0)} B_{\nu_n}^{(-1)} + D_{\nu_n}^{\times(-2)} B_{\nu_n}^{(1)})_{\nu_n}. \tag{4.22}$$

Therefore, it is sufficient to show that the two spectral functions have the same Laurent series coefficients in the -1, 0 and 1st order around $\nu_n = \Delta + n - \frac{d}{4}$. Indeed for a fixed ν_n ,

$$B_{\nu_n}^{k(-1,0)} = 0, \text{ if } k > n. \quad (4.23)$$

Hence by summing up only a finite number of k , it is possible to check explicitly that

$$B^{\text{perturb}(-1,0)}(\nu_n) = \sum_{k=0}^n B_{\nu_n}^{k(-1,0)} = B^{\text{bootstrap}(-1,0)}(\nu_n). \quad (4.24)$$

Since $\gamma_{n,0}^{(2)}$ depends only on $B_{\nu_n}^{(0)}$, one can thus extract the anomalous dimension from a finite number of terms, even though $B^{\text{perturb}}(\nu)$ takes the form of an infinite sum. The s -channel anomalous dimensions is then found to be

$$\gamma_{n,0}^{(2)s} = -\frac{\lambda^2}{256\pi^2(n+1)^3}. \quad (4.25)$$

Concerning the OPE coefficients, we note that $B_{\nu_n}^{k(1)}$ are nonzero at all orders of k and n , so that one does have to solve the infinite sum in order to extract $A_{n,0}^{(2)}$ from $B^{\text{perturb}(-1,0)}(\nu_n) = \sum_{k=0}^{\infty} B_{\nu_n}^{k(1)}$. Nevertheless, by summing up the first few hundreds of terms numerically, we found the approximation to be in agreement with analytic results given by $B^{\text{bootstrap}(-1,0)}(\nu_n)$. The first few entries of $A_{n,0}^{(2)}$ are shown in Table 1.

	$A_{n,0}^{(2)s}$
$n=0$	$-\frac{11}{2} - \frac{\pi^2}{6} + 20 \log 2 - 16 \log^2 2$
$n=1$	$-\frac{163}{128} - \frac{3\pi^2}{32} + \frac{69}{8} \log 2 - 9 \log^2 2$
$n=2$	$-\frac{23751}{131072} - \frac{675\pi^2}{32768} + \frac{1755}{1024} \log 2 - \frac{2025}{1024} \log^2 2$
$n=3$	$-\frac{394619}{18874368} - \frac{1225\pi^2}{393216} + \frac{48335}{196608} \log 2 - \frac{1225}{4096} \log^2 2$
$n=4$	$-\frac{73522975}{34359738368} - \frac{826875\pi^2}{2147483648} + \frac{15789375}{536870912} \log 2 - \frac{2480625}{67108864} \log^2 2$

Table 1. First few OPE coefficients at 2nd order

At this point all are settled with the s - channel. By expanding the elliptic integral we were able to reduce the loop diagram into a sum of tree level diagrams and hence read off its spectral function, due to the close relation between conformal partial wave and the tree level cross diagram. We managed to reproduce existing results of the boundary CFT, although our method, having to deal with a finite (in the case of anomalous dimensions) and infinite (in the case of OPE coefficients) sum, is in no way better than [5]. However, as we shall see soon, in the t and u channel there is no easy way to read off the spectral function. That is when the expansion trick stands out and allow us to obtain similar results through conformal block expansion.

5 Conformal block expansion in the t - and u -channel

Unfortunately, the methodology employed for the s - channel is not directly applicable to the t and u channels. In [5], the spectral function in the s - channel was bootstrapped

using constraints arising from disconnected diagrams. These constraints do not encode information about double-trace operators with spin and are therefore insufficient for bootstrapping the t - and u -channel spectral functions, which involve nontrivial spin exchange. In principle, one may obtain the t - and u -channel CFT data from the s -channel data via the use of 6j symbol (e.g.[24]); however, it is not clear how this can be done in practice. We begin this section by demonstrating that, even when employing the expansion trick (4.9), the spectral function cannot be read off directly. We then proceed in Section 5.2 with an introduction to an algorithm of conformal block expansion, which so far appears to be the only method that allows for a successful extraction of the dual CFT data in the t and u channels. In Section 5.3 conformal block expansion is performed for the s -channel as a consistency check against spectral function. Section 5.4 follows the same procedure to derive the t and u channel contributions to the anomalous dimensions.

5.1 Spectral function does not work easily for t and u channel

Much like (4.9), the t channel loop diagram reads

$$\begin{aligned}
\mathcal{K}_4^t &= \frac{\lambda^2}{4\pi a} \sum_{k=0}^{\infty} C_k (r_{24}^2)^k \mathcal{I}_4\left(\frac{3}{2}, \frac{3}{2} + k, \frac{3}{2}, \frac{3}{2} + k\right) \\
&\quad - \frac{\lambda^2}{4\pi a} \sum_{k=0}^{\infty} D_k \frac{d}{d\epsilon} \Big|_{\epsilon=0} (r_{24}^2)^{k+\epsilon} \mathcal{I}_4\left(\frac{3}{2}, \frac{3}{2} + k + \epsilon, \frac{3}{2}, \frac{3}{2} + k + \epsilon\right) \\
&= \frac{\lambda^2}{4\pi a} \sum_{k=0}^{\infty} C_k (r_{24}^2)^k \int_{\mathbb{R}} d\nu \frac{\nu^2}{\pi} b_{\Delta, \Delta+k, \nu} b_{\Delta+k, \Delta, -\nu} \Psi_{x_1, x_2, x_3, x_4, \nu}^{\Delta, \Delta+k, \Delta, \Delta+k} \\
&\quad - \frac{\lambda^2}{4\pi a} \sum_{k=0}^{\infty} D_k \frac{d}{d\epsilon} \Big|_{\epsilon=0} (r_{24}^2)^{k+\epsilon} \int_{\mathbb{R}} d\nu \frac{\nu^2}{\pi} b_{\Delta, \Delta+k+\epsilon, \nu} b_{\Delta+k+\epsilon, \Delta, -\nu} \Psi_{x_1, x_2, x_3, x_4, \nu}^{\Delta, \Delta+k+\epsilon, \Delta, \Delta+k+\epsilon},
\end{aligned} \tag{5.1}$$

or diagrammatically

$$\begin{array}{c}
 \text{Diagram 1: } \text{A circle with 6 vertices. Vertices at 12, 3, 6, 9, 0, 3 o'clock are black. Vertices at 3, 6, 9, 12 o'clock are white. Edges connect (12,3), (3,6), (6,9), (9,12), (12,6), (3,9), (12,9), (6,3), (9,6), (12,3), (6,9), (9,12), (12,6).} \\
 \text{Diagram 2: } \text{A circle with 6 vertices. Vertices at 12, 3, 6, 9, 0, 3 o'clock are black. Vertices at 3, 6, 9, 12 o'clock are white. Edges connect (12,3), (3,6), (6,9), (9,12), (12,6), (3,9), (12,9), (6,3), (9,6), (12,3), (6,9), (9,12), (12,6).} \\
 \text{Diagram 3: } \text{A circle with 6 vertices. Vertices at 12, 3, 6, 9, 0, 3 o'clock are black. Vertices at 3, 6, 9, 12 o'clock are white. Edges connect (12,3), (3,6), (6,9), (9,12), (12,6), (3,9), (12,9), (6,3), (9,6), (12,3), (6,9), (9,12), (12,6).}
 \end{array}
 = \sum_{k \geq 0} C_k + \sum_{k \geq 0} D_k \frac{d}{d\epsilon} \Big|_{\epsilon=0} + \sum_{k \geq 0} \frac{3}{2} + k + \frac{3}{2} + k + \frac{3}{2} + k + \epsilon + \frac{3}{2} + k + \epsilon \quad (5.2)$$

However, a problem arises that

$$\begin{aligned}
& \Psi_{x_1, x_2, x_3, x_4, \nu}^{\Delta, \Delta+k+\epsilon, \Delta, \Delta+k+\epsilon} \\
&= \int_{\partial \text{AdS}_{d+1}} d^d x_0 \langle \mathcal{O}_\Delta(x_1) \mathcal{O}_{\Delta+k+\epsilon}(x_2) \mathcal{O}_{\frac{d}{2}+i\nu}(x_0) \rangle \langle \mathcal{O}_{\frac{d}{2}-i\nu}(x_0) \mathcal{O}_\Delta(x_3) \mathcal{O}_{\Delta+k+\epsilon}(x_4) \rangle \\
&= \int_{\partial \text{AdS}_{d+1}} d^d x_0 \frac{1}{x_{12}^{2\Delta+k+\epsilon-\Delta(\nu)} x_{10}^{\Delta(\nu)} x_{20}^{\Delta(\nu)}} \frac{1}{x_{34}^{2\Delta+k+\epsilon-\Delta(\nu)} x_{30}^{\Delta(\nu)} x_{40}^{\Delta(\nu)}} \\
&\neq \frac{1}{(r_{24}^2)^{k+\epsilon}} \Psi_{x_1, x_2, x_3, x_4, \nu}^{\Delta, \Delta, \Delta, \Delta}.
\end{aligned} \tag{5.3}$$

Thus, if we consider $\Psi_{x_1, x_2, x_3, x_4, \nu}^{\Delta, \Delta, \Delta, \Delta}$ and $\Psi_{x_1, x_2, x_3, x_4, \nu}^{\Delta, \Delta+k+\epsilon, \Delta, \Delta+k+\epsilon}$ each as an infinite dimensional set of basis indexed by ν spanning the space of all four point correlators, there is no diagonal transformation matrix between these two sets of basis, unlike the case of $\Psi^{\Delta, \Delta, \Delta+k+\epsilon, \Delta+k+\epsilon}$ in the s -channel. Hence we cannot easily read off the spectral function while having the s -channel conformal partial waves as basis, which is a prerequisite for obtaining dual CFT information with respect to the s -channel conformal block. For this reason we will have to resort to the method of conformal block expansion as performed in [4, 8, 9, 25].

5.2 Conformal Block Expansion

Since, unlike of the s -channel, the spectral function for the t - and u -channel cannot be read off directly from the respective expressions of the bubble Feynman integrals, in this section we will resort to the method of conformal block expansion as performed in [4] [9] [8] [25]. Comparison between (2.18) and

$$\begin{aligned}
\langle \bar{\phi}(x_1) \bar{\phi}(x_2) \bar{\phi}(x_3) \bar{\phi}(x_4) \rangle &= \text{(Diagram 1)} + \text{(Diagram 2)} + \text{(Diagram 3)} \\
&+ \lambda \text{(Diagram 4)} + \frac{\lambda^2}{2} \left(\text{(Diagram 5)} + \text{(Diagram 6)} + \text{(Diagram 7)} \right) + \mathcal{O}(\lambda^3) \\
&:= \frac{N_\phi^2}{(r_{12} r_{34})^{2\Delta}} \left[1 + u^\Delta + \frac{u^\Delta}{v^\Delta} + \lambda \mathcal{I}_4 + \frac{\lambda^2}{2} (\mathcal{K}_4^s + \mathcal{K}_4^t + \mathcal{K}_4^u) \right] + \mathcal{O}(\lambda^3),
\end{aligned} \tag{5.4}$$

enables us to extract $\gamma_{n,l}^{(1)}$, $\gamma_{n,l}^{(2)}$, $A_{n,l}^{(1)}$ and $A_{n,l}^{(2)}$. Individual terms are compared in the following order:

1. $W_{\mathcal{O}(\log u)}^\times := \left(\gamma_{n,l}^{(1)} A_{n,l} G'_{n,l} \right)_{\mathcal{O}(\log u)}$, starting from $n = l = 0$. $\gamma_{n,l}^{(1)}$ could then be determined recursively. To determine a higher order $\gamma_{N,L}^{(1)}$, knowledge from previous iterations of all $\gamma_{n,l}^{(1)}$ with $n < N$ and $l < L$ is required. More details on this recursive algorithm can be found in Appendix C.
2. $W_{\mathcal{O}(1)}^\times := \gamma_{n,l}^{(1)} \left(A_{n,l} G'_{n,l} + C_{n,l}^{(1)} G_{n,l} \right)_{\mathcal{O}(1)}$, so that $A_{n,l}^{(1)}$ are determined recursively.

3. $W_{\mathcal{O}(\log^2 u)}^{\nearrow} := \left(\frac{1}{2}(\gamma_{n,l}^{(1)})^2 A_{n,l} G_{n,l}'' \right)_{\mathcal{O}(\log^2 u)}$, so that $\gamma_{n,l}^{(1)}$ is again determined independently. This provides us with a consistency check, which is equivalent to (B.22) and [5, 4.24], that enables the spectral function of the loop diagram to be bootstrapped.
4. $W_{\mathcal{O}(\log u)}^{\nearrow} := \left(\gamma_{n,l}^{(2)} A_{n,l} G_{n,l}' \right)_{\mathcal{O}(\log u)}$, so that $A_{n,l}^{(2)}$ are determined recursively.
5. $W_{\mathcal{O}(1)}^{\nearrow} := \left(\gamma_{n,l}^{(2)} \left(A_{n,l} G_{n,l}' + A_{n,l}^{(1)} G_{n,l} \right) \right)_{\mathcal{O}(1)}$, so that $A_{n,l}^{(2)}$ are determined recursively.

Furthermore, since $\gamma_{n,l}^{(2)}$ and $A_{n,l}^{(2)}$ appear in the conformal block expansion only up to linear order, it is possible to split them into

$$\gamma_{n,l}^{(2)} = \gamma_{n,l}^{(2)s} + \gamma_{n,l}^{(2)t} + \gamma_{n,l}^{(2)u} \quad (5.5)$$

and

$$A_{n,l}^{(2)} = A_{n,l}^{(2)s} + A_{n,l}^{(2)t} + A_{n,l}^{(2)u}, \quad (5.6)$$

so that loop corrections in s -, t - and u - channels correspond with the conformal block expansion,

$$\begin{aligned} W_s^{\nearrow} := & \frac{1}{2}(\gamma_{n,l}^{(1)})^2 \left(A_{n,l} G_{\Delta(n,l),l}'' + A_{n,l}^{(2)s} G_{\Delta(n,l),l} + 2A_{\Delta(n,l),l}^{(1)} G_{\Delta(n,l),l}' \right) \\ & + (\gamma_{n,l}^{(2)s}) \left(A_{n,l} G_{\Delta(n,l),l}'' + A_{n,l}^{(1)} G_{\Delta(n,l),l} \right) \end{aligned} \quad (5.7)$$

and

$$\begin{aligned} W_{t,u}^{\nearrow} := & \frac{1}{2}(\gamma_{n,l}^{(1)})^2 A_{n,l}^{(2)t,u} G_{\Delta(n,l),l} \\ & + (\gamma_{n,l}^{(2)t,u}) \left(A_{n,l} G_{\Delta(n,l),l}'' + A_{n,l}^{(1)} G_{\Delta(n,l),l} \right). \end{aligned} \quad (5.8)$$

The splitting of $\gamma_{n,l}^{(2)}$ and $A_{n,l}^{(2)}$ creates redundant degrees of freedom. As seen in (5.7) and (5.8), we decided to have $A_{n,l}^{(2)s}$ and $\gamma_{n,l}^{(2)s}$ compensate for $\frac{1}{2}(\gamma_{n,l}^{(1)})^2 (A_{n,l} G_{\Delta(n,l),l}'' + 2A_{\Delta(n,l),l}^{(1)} G_{\Delta(n,l),l}')$ entirely, so that they fit also with [5] for an $\mathcal{O}(\mathcal{N})$ model at large \mathcal{N} limit. However, one is free to redistribute this compensation among all 3 channels.

5.3 The s channel as a warm-up

As a first example of conformal block expansion we begin again with the s -channel diagram

Since $\Delta_1 + \Delta_2 \neq \Delta_3 + \Delta_4$, we insert (3.6) and [22, B.11] into (4.9) and find

$$\begin{aligned}
\mathcal{K}_4^s &= \frac{\lambda^2}{4\pi a} \sum_{k=0}^{\infty} C_k (r_{34}^2)^k \mathcal{I}_4\left(\frac{3}{2}, \frac{3}{2}, \frac{3}{2} + k, \frac{3}{2} + k\right) \\
&\quad - \frac{\lambda^2}{4\pi a} \sum_{k=0}^{\infty} D_k \frac{d}{d\epsilon} \Big|_{\epsilon=0} (r_{34}^2)^{k+\epsilon} \mathcal{I}_4\left(\frac{3}{2}, \frac{3}{2}, \frac{3}{2} + k + \epsilon, \frac{3}{2} + k + \epsilon\right) \\
&= \lim_{\epsilon \rightarrow 0} \left(\frac{\lambda^2}{4\pi a} \sum_{k=0}^{\infty} C_k \frac{1}{(r_{13})^3 (r_{24})^3} \frac{\pi}{\Gamma(\frac{3}{2})^2 \Gamma(\frac{3}{2} + k)^2} \left(\frac{a}{2\pi}\right)^4 \frac{\Gamma(3+k-1)}{2} (H_1^{k+\epsilon} + H_2^{k+\epsilon}) \right. \\
&\quad \left. - \frac{\lambda^2}{4\pi a} \sum_{k=0}^{\infty} D_k \frac{d}{d\epsilon} \frac{1}{(r_{13})^3 (r_{24})^3} \frac{\pi}{\Gamma(\frac{3}{2})^2 \Gamma(\frac{3}{2} + k + \epsilon)^2} \left(\frac{a}{2\pi}\right)^4 \frac{\Gamma(3+k+\epsilon-1)}{2} (H_1^{k+\epsilon} + H_2^{k+\epsilon}) \right), \tag{5.9}
\end{aligned}$$

where we recall from (4.11) and used its first equality, with $H(\alpha, \beta, \gamma, \delta; u, v) = H_1(\alpha, \beta, \gamma, \delta; u, v) + H_2(\alpha, \beta, \gamma, \delta; u, v)$ whose explicit expression is given by [22, 5.9]. Concretely we have

$$\begin{aligned}
H_1^{k+\epsilon} &= H_1\left(\frac{3}{2}, \frac{3}{2}, 1-k-\epsilon, 3; u, v\right) = \frac{\Gamma(k+\epsilon)}{2} \left(\Gamma\left(\frac{3}{2}\right)\right)^4 G\left(\frac{3}{2}, \frac{3}{2}, 1-k-\epsilon, 3; u, 1-v\right), \\
&:= \sum_{m,n=0}^{\infty} H_1^{k+\epsilon, m, n} u^m (1-v)^n
\end{aligned} \tag{5.10}$$

and

$$\begin{aligned}
H_2^{k+\epsilon} &= H_2\left(\frac{3}{2}, \frac{3}{2}, 1-k-\epsilon, 3; u, v\right) \\
&= \frac{\Gamma(-k-\epsilon)}{\Gamma(3+2k+2\epsilon)} \left(\Gamma\left(\frac{3}{2}+k+\epsilon\right)\right)^2 \left(\Gamma\left(\frac{7}{2}+k+\epsilon\right)\right)^2 \\
&\quad \times u^{k+\epsilon} G\left(\frac{3}{2}+k+\epsilon, \frac{3}{2}+k+\epsilon, 1+k+\epsilon, 3+2k+2\epsilon; u, 1-v\right) \\
&:= \sum_{m,n=0}^{\infty} u^{k+\epsilon} \times H_2^{k+\epsilon, m, n} u^m (1-v)^n,
\end{aligned} \tag{5.11}$$

while the function G is defined in [22, 5.1] as

$$G(\alpha, \beta, \gamma, \delta; x, y) = \sum_{m,n=0}^{\infty} \frac{(\delta-\alpha)_m (\delta-\beta)_m}{m! (\gamma)_m} \frac{(\alpha)_{m+n} (\beta)_{m+n}}{n! (\delta)_{2m+n}} x^m y^n. \tag{5.12}$$

The factor of $u^{k+\epsilon}$ in (5.11) is of particular importance here. As this factor increases the power of u by k after taking the $\epsilon \rightarrow 0$ limit, for any fixed i and j , contributions from $H_2^{k+\epsilon}$ to the $u^i (1-v)^j$ term in \mathcal{K}_4^s could only come from those $H_2^{k+\epsilon, m, n}$ with $m+k < i$. Hence we rewrite

$$\mathcal{K}_4^s = \lim_{\epsilon \rightarrow 0} \frac{\lambda^2}{128\pi^4} \frac{1}{(r_{13})^3 (r_{24})^3} \sum_{i,j=0}^{\infty} \left(H_{\log}^{i,j} + H_{\text{nonlog}}^{i,j} \right) u^i (1-v)^j \tag{5.13}$$

where

$$H_{\log}^{i,j} = \sum_{k=0}^i \left(C_k \frac{\Gamma(2+k)}{\Gamma(\frac{3}{2}+k+\epsilon)^2} (H_1^{k+\epsilon,i,j} + H_2^{k+\epsilon,i-k,j}) + D_k \frac{d}{d\epsilon} \frac{\Gamma(2+k+\epsilon)}{\Gamma(\frac{3}{2}+k+\epsilon)^2} (H_1^{k+\epsilon,i,j} + H_2^{k+\epsilon,i-k,j}) \right), \quad (5.14)$$

and

$$H_{\text{nonlog}}^{i,j} = \sum_{k=i+1}^{\infty} C_k \frac{\Gamma(2+k)}{\Gamma(\frac{3}{2}+k+\epsilon)^2} H_1^{k+\epsilon,i,j}. \quad (5.15)$$

As the $\epsilon \rightarrow 0$ limit is taken, the finite sum $H_{\log}^{i,j}$ gives rise to terms proportional to $\log u$ and $\log^2 u$, while the infinite sum $H_{\text{nonlog}}^{i,j}$ contributes to terms without $\log u$. The anomalous dimension is determined by the $\log u$ and $\log^2 u$ terms only, while the OPE coefficient is determined by terms without $\log u$ too. This is consistent with the observation in (4.24) that the anomalous dimensions can be written as a finite sum, but the OPE coefficients cannot. Plugging the explicit expression of \mathcal{K}_4^s back into (2.18), we obtained again the exact values of the anomalous dimensions (4.25), and the OPE coefficients by numeric approximation in Table 1.

5.4 t - and u - channel anomalous dimensions

For the t - and u -channel, $\Delta_1 + \Delta_2 = \Delta_3 + \Delta_4$, or in the convention of [22, 5.13], $\gamma = 1$. We therefore plug in instead [22, 5.13] into (4.9), and use the second identity in (4.11), resulting in

$$\mathcal{K}_4^{t|u,\log} = \sum_{m,n,k=0}^{\infty} \frac{1}{128\pi^4} K_+^{t|u,m,n,k} u^m (1-v)^n, \quad (5.16)$$

in which

$$K_+^{t,m,n,k} = \frac{4(1+k) \Gamma(\frac{3}{2}+m) \Gamma(\frac{3}{2}+k+m) \Gamma(\frac{3}{2}+m+n) \Gamma(\frac{3}{2}+k+m+n)}{(1+2k) \pi^2 \Gamma(2+k) \Gamma(1+m)^2 \Gamma(1+n) \Gamma(3+k+2m+n)} \times \left(-\frac{2}{1+2k} - H_k + H_{\frac{1}{2}+k+m} + H_{\frac{1}{2}+k+m+n} - H_{2+k+2m+n} \right) \quad (5.17)$$

and

$$K_+^{u,m,n,k} = \frac{4 \Gamma(\frac{3}{2}+k+m)^2 \Gamma(\frac{3}{2}+m+n)^2}{(1+2k)^2 \pi^2 \Gamma(1+k) \Gamma(1+m)^2 \Gamma(1+n) \Gamma(3+k+2m+n)} \times \left(-2 + (-1-2k) H_k + (2+4k) H_{\frac{1}{2}+k+m} + (-1-2k) H_{2+k+2m+n} \right), \quad (5.18)$$

where H_k are the harmonic numbers. It turns out that we may evaluate the infinite sum over k with a clever trick: We define

$$K_-^{t,m,n,k} = \frac{4(1+k) \Gamma(\frac{3}{2}+m) \Gamma(\frac{3}{2}+k+m) \Gamma(\frac{3}{2}+m+n) \Gamma(\frac{3}{2}+k+m+n)}{(1+2k) \pi^2 \Gamma(2+k) \Gamma(1+m)^2 \Gamma(1+n) \Gamma(3+k+2m+n)} \times \left(-\frac{2}{1+2k} - H_k + H_{\frac{1}{2}+k+m} - H_{\frac{1}{2}+k+m+n} + H_{2+k+2m+n} \right), \quad (5.19)$$

and

$$K_-^{u,m,n,k} = \frac{4 \Gamma\left(\frac{3}{2} + k + m\right)^2 \Gamma\left(\frac{3}{2} + m + n\right)^2}{(1+2k)^2 \pi^2 \Gamma(1+k) \Gamma(1+m)^2 \Gamma(1+n) \Gamma(3+k+2m+n)} \times (-2 - (-1-2k) H_k + (-1-2k) H_{2+k+2m+n}), \quad (5.20)$$

which differs from $K_+^{t,m,n,k}$, $K_-^{u,m,n,k}$ in (5.16) and (5.18) by two relative minus signs. Furthermore, we denote $K_{\pm}^{t|u,m,n} = \sum_{k=0}^{\infty} K_{\pm}^{t|u,m,n,k}$. The evaluation of the infinite sums over k then relies on the following conjectures.

Conjecture 5.1. *For any $m, n \in \mathbb{Z}$, $K_-^{t|u,m,n}$ can be uniquely written as $q_1 + \frac{q_2}{\pi}$, in which $q_1, q_2 \in \mathbb{Q}$.*

Conjecture 5.2. $K_+^{t|u,m,n} = q_1$.

With the help of Mathematica we were able to compute the infinite sum $K_-^{t,m,n}$ and $K_-^{u,m,n}$ exactly. It is then verified that q_1 is in agreement with the numerical approximation of $K_+^{t|u,m,n}$. $K_+^{t|u,m,n}$ are then computed in this way on a computer cluster for all m and even n with $m+2n \leq 100$.

$K_+^{t|u,m,n}$ with odd n are not helpful to the determination of anomalous dimensions, since they contain information of $(\gamma_{n,l}^{(2)t|u}) A_{n,l} G'_{\Delta(n,l),l}$ with l strictly smaller than n . That is, they do not provide any new information during the recursive iterations, other than those already known from even n terms. Later on however, after obtaining $\gamma_{n,l}^{(2)t|u}$ from (5.22), a consistency check can be performed by plugging $\gamma_{n,l}^{(2)t|u}$ back into the conformal block expansion. This indeed reproduced $K_+^{t|u,m,n}$ for odd n as well. It shows that the correlation function correctly admits a conformal block expansion, despite us not being entirely rigorous when we computed the infinite sum over k .

The $\mathcal{O}(\log u)$ contribution to the conformal block expansion at $\mathcal{O}(\lambda^2)$ comes from

$$\begin{aligned} & (\mathcal{A}_{n,l} \mathcal{G}_{\Delta(n,l),l})_{\mathcal{O}(\lambda^2), \mathcal{O}(\log u)} \\ &= \left(\frac{1}{2} (\gamma_{n,l}^{(1)}(\Delta))^2 2 A_{\Delta(n,l),l}^{(1)} G'_{\Delta(n,l),l} + (\gamma_{n,l}^{(2)s}(\Delta)) A_{n,l} G'_{\Delta(n,l),l} \right)_{\mathcal{O}(\log u)}. \end{aligned} \quad (5.21)$$

To evaluate $\gamma_{n,l}^{(2)t|u}(\Delta)$, we manually set $\gamma_{n,l}^{(1)}(\Delta) = 0$ during the t and u channel iterations, since $\frac{1}{2} (\gamma_{n,l}^{(1)}(\Delta))^2 2 A_{\Delta(n,l),l}^{(1)} G'_{\Delta(n,l),l}$ has been fully accounted for in the s -channel. This leaves us with

$$W_{t|u, \mathcal{O}(\log u)}^{\propto} = \left((\gamma_{n,l}^{(2)t|u}) A_{n,l} G'_{\Delta(n,l),l} \right)_{\mathcal{O}(\log u)}. \quad (5.22)$$

Then, $\gamma_{n,l}^{(2)t|u}$ are determined recursively for all even l and $2n+l \leq 100$. These numbers were fed to the Guess package as part of the RISCergoSUM package [26, 27], with which a recursive relation was found for $\gamma_{n,l}^{(2)t} + \gamma_{n,l}^{(2)u}$, given the initial values. This important result allows us to evaluate the anomalous dimensions for any n and l which is not available in any previous literature to our knowledge. Since the explicit form of this recursion is somewhat

$\gamma_{n,l}^t$	$l = 0$	$l = 2$	$l = 4$	$l = 6$	$l = 8$
$n = 0$	$-\frac{\lambda^2}{192\pi^2}$	$\frac{5\lambda^2}{4032\pi^2}$	$-\frac{299\lambda^2}{24640\pi^2}$	$\frac{68861\lambda^2}{172480\pi^2}$	$-\frac{347063483\lambda^2}{12640320\pi^2}$
$n = 1$	$-\frac{\lambda^2}{5040\pi^2}$	$-\frac{4777\lambda^2}{221760\pi^2}$	$\frac{710383\lambda^2}{720720\pi^2}$	$-\frac{160778091931\lambda^2}{1862340480\pi^2}$	$\frac{29966280403819\lambda^2}{2433740400\pi^2}$
$n = 2$	$-\frac{811973\lambda^2}{29937600\pi^2}$	$\frac{4932359\lambda^2}{2882880\pi^2}$	$-\frac{19107541407709\lambda^2}{97772875200\pi^2}$	$\frac{59710558672625843\lambda^2}{1734770157120\pi^2}$	$-\frac{91522523466052657037\lambda^2}{10601373182400\pi^2}$
$n = 3$	$-\frac{20709259\lambda^2}{10090080\pi^2}$	$-\frac{110254681709\lambda^2}{349188840\pi^2}$	$\frac{1503137554547357\lambda^2}{21416915520\pi^2}$	$-\frac{29911835316920716043\lambda^2}{1405485081000\pi^2}$	$\frac{222834973307634513509129\lambda^2}{26369344441440\pi^2}$
$n = 4$	$-\frac{2711482461412687\lambda^2}{7332965640000\pi^2}$	$\frac{5035734323168371943\lambda^2}{47224298721600\pi^2}$	$-\frac{237059057696361975071\lambda^2}{5952642696000\pi^2}$	$\frac{627127244738145656083221381\lambda^2}{333572207184216000\pi^2}$	$-\frac{3330235595179796001428378445023\lambda^2}{30324746107656000\pi^2}$

Table 2. Some lowest order $\gamma_{n,l}^{(2),t}$

$\gamma_{n,l}^u$	$l = 0$	$l = 2$	$l = 4$	$l = 6$	$l = 8$
$n = 0$	$-\frac{\lambda^2}{192\pi^2}$	$-\frac{31\lambda^2}{20160\pi^2}$	$\frac{2677\lambda^2}{221760\pi^2}$	$-\frac{2685733\lambda^2}{6726720\pi^2}$	$\frac{5900076901\lambda^2}{214885440\pi^2}$
$n = 1$	$-\frac{37\lambda^2}{10080\pi^2}$	$\frac{131\lambda^2}{6160\pi^2}$	$-\frac{4262627\lambda^2}{4324320\pi^2}$	$\frac{10048627093\lambda^2}{116396280\pi^2}$	$-\frac{59932560885053\lambda^2}{4867480800\pi^2}$
$n = 2$	$-\frac{750203\lambda^2}{29937600\pi^2}$	$-\frac{10570753\lambda^2}{6177600\pi^2}$	$\frac{6369178024393\lambda^2}{32590958400\pi^2}$	$-\frac{59710558731540149\lambda^2}{1734770157120\pi^2}$	$\frac{18304504693171821479\lambda^2}{2120274636480\pi^2}$
$n = 3$	$-\frac{2072237\lambda^2}{1009008\pi^2}$	$\frac{73503077213\lambda^2}{232792560\pi^2}$	$-\frac{751568778021689\lambda^2}{10708457760\pi^2}$	$\frac{59823670633746001289\lambda^2}{2810970162000\pi^2}$	$-\frac{4271003655063004511982203\lambda^2}{505412435127600\pi^2}$
$n = 4$	$-\frac{271147585567217\lambda^2}{7332965640000\pi^2}$	$-\frac{1007146866120317821\lambda^2}{9444859744320\pi^2}$	$\frac{16584378521941152371\lambda^2}{416440024000\pi^2}$	$-\frac{627127244738156592681917019\lambda^2}{333572207184216000\pi^2}$	$\frac{333023559517979600845938497969\lambda^2}{30324746107656000\pi^2}$

Table 3. Some lowest order $\gamma_{n,l}^{(2),u}$

$\gamma_{n,l}$	$l = 0$	$l = 2$	$l = 4$	$l = 6$	$l = 8$
$n = 0$	$-\frac{11\lambda^2}{768\pi^2}$	$-\frac{\lambda^2}{3360\pi^2}$	$-\frac{\lambda^2}{15840\pi^2}$	$-\frac{\lambda^2}{43680\pi^2}$	$-\frac{\lambda^2}{93024\pi^2}$
$n = 1$	$-\frac{937\lambda^2}{215040\pi^2}$	$-\frac{61\lambda^2}{221760\pi^2}$	$-\frac{47\lambda^2}{617760\pi^2}$	$-\frac{253\lambda^2}{8062080\pi^2}$	$-\frac{397\lambda^2}{24961440\pi^2}$
$n = 2$	$-\frac{17627\lambda^2}{7983360\pi^2}$	$-\frac{4943\lambda^2}{21621600\pi^2}$	$-\frac{104779\lambda^2}{1396755360\pi^2}$	$-\frac{297547\lambda^2}{8761465440\pi^2}$	$-\frac{676747\lambda^2}{37067738400\pi^2}$
$n = 3$	$-\frac{1004021\lambda^2}{738017280\pi^2}$	$-\frac{131779\lambda^2}{698377680\pi^2}$	$-\frac{1496021\lambda^2}{21416915520\pi^2}$	$-\frac{1239361\lambda^2}{36506106000\pi^2}$	$-\frac{57960383\lambda^2}{3029445165600\pi^2}$
$n = 4$	$-\frac{86793659\lambda^2}{93117024000\pi^2}$	$-\frac{58993787\lambda^2}{374796021600\pi^2}$	$-\frac{460967861\lambda^2}{7228208988000\pi^2}$	$-\frac{23672291549\lambda^2}{722017764468000\pi^2}$	$-\frac{13867617787\lambda^2}{722017764468000\pi^2}$

Table 4. Some lowest order $\gamma_{n,l}^{(2),s+t+u}$

lengthy, we describe it in detail in Appendix D. With it, the computation time required for $2n + l \approx 100$ was reduced from thousands of hours (that of computing the sum $K_{-}^{t,m,n}$ with Mathematica directly), to merely a few seconds. Some of the first anomalous dimensions are also shown in Table 2 and Table 3. Combining them with (4.25), we obtained the total contribution from all channels to the anomalous dimensions, some of the first entries shown in Table 4.

An interesting feature that emerged in our analysis is a fine-tuning-like behavior in the t - and u -channel anomalous dimensions. In particular, at large $2n + l$ limit, the combined contribution $\gamma_{n,l}^{(2),t+u}$ is magnitudes of order smaller than the individual contributions $\gamma_{n,l}^{(2),t}$ and $\gamma_{n,l}^{(2),u}$ (at $2n + l \sim 100$, this magnitude could be up to 10^{200}). While (5.6) introduces

redundant degrees of freedom in the separate definitions of $\gamma_{n,l}^{(2),t}$ and $\gamma_{n,l}^{(2),u}$ such that only their sum represents a physical quantity, we nevertheless speculate that this 'fine-tuning' may be related to an underlying symmetry shared by the two channels. It would be interesting to investigate whether this behavior admits an interpretation in terms of the $6j$ symbols. We leave a detailed exploration of this possibility to future work.

In addition, for $n = 0$ we were able to guess a closed form for the anomalous dimensions as a function of l :

$$\gamma_{0,l}^{s+t+u} = -\frac{\lambda^2}{32\pi^2(l+1)(2l+1)(2l+3)} - \frac{\lambda^2}{256\pi^2}\delta^{l0}. \quad (5.23)$$

This is another key result of this paper. If we substitute the intrinsic spin l with the conformal spin J , defined as

$$J^2 = (l + \tau/2)(l + \tau/2 - 1) = \left(l + \frac{3}{2}\right)\left(l + \frac{1}{2}\right), \quad (5.24)$$

where $\tau = 2\Delta = 3$, the anomalous dimensions become

$$\begin{aligned} \gamma_{0,l}^{s+t+u} &= \frac{1}{64\pi^4 J^2 \sqrt{1 + 4J^2}} \\ &= \frac{1}{128\pi^4} \left(\frac{1}{J^3} - \frac{1}{8J^5} + \frac{3}{128J^7} - \frac{5}{1024J^9} + \frac{35}{32768J^{11}} + \mathcal{O}(J^{-13}) \right) \end{aligned} \quad (5.25)$$

when expanded at large J limit. The series in J contains only $\frac{1}{J^\tau}$ times even power terms of J , which agrees with [28–31]. To summarize, using a new representation of one loop diagrams in terms of an infinite sum of tree level diagrams, combined with some intricate manipulations of these infinite sums inside the conformal block expansion, we were able to extract a recursion relation for all second order anomalous dimensions of the deformed 2-dimensional conformal field theory corresponding to an interacting scalar field theory in AdS_3 .

6 Conclusion

In this paper, we computed the four-point one-loop correlator of a conformally coupled ϕ^4 interacting scalar field in AdS_3 . Direct evaluation of the associated Feynman integrals proved challenging due to the non-integer powers arising from the conformal dimension of the field. However, we found that the one-loop correlator admits a series expansion in tree-level 'cross' diagrams with progressively increasing conformal dimensions in the bulk-to-boundary propagators.

In the s -channel, this discovery allows the spectral function of the loop diagram to be expressed as a sum of cross-diagram spectral functions. From this spectral function, we extracted the anomalous dimensions and OPE coefficients dual to the bulk one-loop corrections, finding agreement with a different representation of the spectral function obtained by bootstrap. In contrast, this approach fails in the t - and u -channels due to a mismatch in the conformal partial waves. To overcome this obstacle, we instead performed conformal block expansion for each cross diagram appearing in the series. The infinite

sum of cross diagrams was evaluated under the assumption of two conjectures proposed in this work, which allowed us to obtain exact values of the anomalous dimensions in the t - and u -channels. Moreover, we identified a recursive relation that enables the efficient computation of anomalous dimensions at arbitrarily high orders given a few initial values.

Looking ahead, it would be interesting to extend this analysis to the alternative conformally coupled scalar with $\Delta = \frac{1}{2}$ and explore possible connections to known two-dimensional conformal field theories. Another promising direction is to investigate potential links between the framework developed here and recent approaches to cosmological correlators.

Acknowledgments

W.X. would like to thank the China Scholarship Council for sponsoring his doctoral study. W.X. would also like to thank Daniel Bockisch, Eugenia Boffo, Ka Hei Choi, Carlo Alberto Cremonini, Zhen Gao, Jonathan Gräfe, Matthias Nowinski and Dayuan Wang for discussions. Specifically, W.X. would like to thank Till Heckelbacher for supervision of his master project, from which the present work is developed. This work is supported by the Excellence Cluster Origins of the DFG under Germany's Excellence Strategy EXC-2094 390783311 as well as EXC 2094/2: ORIGINS 2.

A Loop calculation

We discuss in detail the calculation of the fish diagram

$$\mathcal{J}_4 = \int d^3y \sqrt{|g_y|} \Lambda(x, y)^2 \bar{\Lambda}(y, x_3) \bar{\Lambda}(y, x_4), \quad (\text{A.1})$$

shown in Figure 2. Similar to [4], the following isometries are applied to simplify the integration:

1. Translation of x, x_3, x_4 by $(-x_4^i, 0)$, denoted by the first prime, such that $x'_4 = (0, 0)$.
2. Inversion of x', y, x'_3, x'_4 , denoted by the second prime, such that

$$K_{x'y} = K_{x''y''} \quad \bar{K}_{x'_3y} = \frac{1}{x'^2} \bar{K}_{x''_3y''} = \frac{1}{r_{34}^2} \bar{K}_{x''_3y''} \quad \bar{K}_{x'_4y} = x''_4^2 \bar{K}_{x''_4y''} = 2w''. \quad (\text{A.2})$$

3. Translation $(y^i, w) = (y''^i - x''^i, w'')$, as well as denoting $x'''_3 = x''_3^i - x''^i$.

The fish diagram then reads

$$\begin{aligned} \mathcal{J}_4 = & \int d^3y \frac{a}{128\pi^4} \frac{1}{r_{34}^3} (z_3 z_4)^{\frac{3}{2}} \left(\frac{1}{(y - x''_3)^2 + w^2} \right)^{\frac{3}{2}} \left(\frac{2wz''}{y^2 + (w - z'')^2} \right. \\ & \left. + \frac{2wz''}{y^2 + (w + z'')^2} - 2\sqrt{\frac{2wz''}{y^2 + (w - z)^2} \frac{2wz}{y^2 + (w + z'')^2}} \right) \\ & := \mathcal{J}_4^1 + \mathcal{J}_4^2 - \mathcal{J}_4^3, \end{aligned} \quad (\text{A.3})$$

where the three terms are to be computed separately.

$$\begin{aligned}\mathcal{J}_4^1 &= \int d^3y \frac{a}{128\pi^4} \frac{1}{r_{34}^3} (z_3 z_4)^{\frac{3}{2}} \left(\frac{1}{(y - x_3''')^2 + w^2} \right)^{\frac{3}{2}} \frac{2wz''}{y^2 + (w - z'')^2} \\ &= \int d^3y C \left(\frac{1}{(y - x_3)^2 + w^2} \right)^{\frac{3}{2}} \frac{w}{y^2 + (w - z'')^2},\end{aligned}\quad (\text{A.4})$$

in which $C = \frac{az''}{64\pi^4} \frac{1}{r_{34}^3} (z_3 z_4)^{\frac{3}{2}}$. Next we make use of the Schwinger parametrization to get

$$\mathcal{J}_4^1 = \int_0^\infty dw dt_1 dt_2 C \frac{1}{\Gamma(\frac{3}{2})} \frac{1}{t_1 + t_2} \pi \sqrt{t_1} w e^{-\frac{t_1^2 w^2 + t_2^2 (w - z'')^2 + t_1 t_2 (2w^2 + x_3''^2 - 2wz'' + z''^2)}{t_1 + t_2}}. \quad (\text{A.5})$$

A change of variable is then made substituting $t_i = ss_i$, and $dt_1 dt_2 = s ds_1 ds_2$. The integration is then performed in the order of $s \rightarrow w \rightarrow s_2$,

$$\begin{aligned}\mathcal{J}_4^1 &= \int dw ds ds_1 ds_2 C \frac{1}{\Gamma(\frac{3}{2})} \delta(1 - s_1 - s_2) \pi s \sqrt{s_1 * s} w \\ &\quad e^{-s(s_1^2 w^2 + s_2^2 (w - z'')^2 + s_1 s_2 (2w^2 + x_3''^2 - 2wz'' + z''^2))} \\ &= \int_0^1 ds_1 C \frac{1}{\Gamma(\frac{3}{2})} \frac{\pi^{3/2} (z'' - s_1 z'' + \sqrt{(1 - s_1) (s_1 x_3''^2 + z''^2)})}{2(1 - s_1) \sqrt{s_1} (x_3''^2 + z''^2)}. \end{aligned}\quad (\text{A.6})$$

Similarly,

$$\mathcal{J}_4^2 = \int_0^1 ds_1 C \frac{1}{\Gamma(\frac{3}{2})} \frac{\pi^{3/2} (s_1 z'' - z'' + \sqrt{(1 - s_1) (s_1 x_3''^2 + z''^2)})}{2(1 - s_1) \sqrt{s_1} x_3''^2}, \quad (\text{A.7})$$

so that

$$\begin{aligned}\mathcal{J}_4^1 + \mathcal{J}_4^2 &= \int_0^1 dt C \frac{1}{\Gamma(\frac{3}{2})} \frac{2\pi^{3/2} (\sqrt{(1 - t^2) (t^2 (x_3''^2) + z''^2)})}{(1 - t^2) x_3''^2} \\ &= C \frac{1}{\Gamma(\frac{3}{2})} \frac{2\pi^{3/2} z'' \text{EllipticE}[-\frac{x_3''^2}{z''^2}]}{x_3''^2 + z''^2}.\end{aligned}\quad (\text{A.8})$$

Finally,

$$\begin{aligned}\mathcal{J}_4^3 &= 2 \int d^3y \frac{a}{128\pi^4} \frac{1}{r_{34}^3} (z_3 z_4)^{\frac{3}{2}} \left(\frac{1}{(y - x_3''')^2 + w^2} \right)^{\frac{3}{2}} \sqrt{\frac{2wz''}{y^2 + (w - z'')^2}} \sqrt{\frac{2wz''}{y^2 + (w + z'')^2}} \\ &= 2 \int dw dt_1 dt_2 dt_3 C \frac{1}{\Gamma(\frac{3}{2})} \frac{1}{\Gamma(\frac{1}{2})} \frac{1}{\Gamma(\frac{1}{2})} \frac{\pi \sqrt{t_1} w}{\sqrt{t_2} \sqrt{t_3} (t_1 + t_2 + t_3)} \\ &\quad e^{-\frac{t_1^2 w^2 + t_2^2 (w - z'')^2 + t_3^2 (w + z'')^2 + 2t_2 t_3 (w^2 + z''^2) + t_1 (t_2 (2w^2 + x_3''^2 - 2wz'' + z''^2) + t_3 (2w^2 + x_3''^2 + 2wz'' + z''^2))}{t_1 + t_2 + t_3}}.\end{aligned}\quad (\text{A.9})$$

Substituting $t_i = ss_i$, $dt_1 dt_2 dt_3 = s^2 ds ds_1 ds_2 ds_3$, and performing integration in the order of $s \rightarrow w \rightarrow s_1$,

$$\begin{aligned}
\mathcal{J}_4^3 &= 2 \int dw ds ds_1 ds_2 ds_3 C \frac{1}{\Gamma(\frac{3}{2})} \frac{1}{\Gamma(\frac{1}{2})} \frac{1}{\Gamma(\frac{1}{2})} \frac{\pi \sqrt{ss_1} w}{\sqrt{s_2} \sqrt{s_3}} \delta(1 - s_1 - s_2 - s_3) \\
&\quad e^{-s(s_1^2 w^2 + s_1((s_2 + s_3)(2w^2 + x_3''^2) + 2(-s_2 + s_3)wz'' + (s_2 + s_3)z''^2) + (s_2 + s_3)(s_2(w - z'')^2 + s_3(w + z'')^2))} \\
&= 2 \int^{0 \leq s_2 + s_3 \leq 1} ds_2 ds_3 C \frac{1}{\Gamma(\frac{3}{2})} \frac{1}{\Gamma(\frac{1}{2})} \frac{1}{\Gamma(\frac{1}{2})} \pi^{3/2} \sqrt{1 - s_2 - s_3} \\
&\quad \frac{(s_2 - s_3)z'' + \sqrt{(s_2 + s_3)((1 - s_2 - s_3)x_3''^2 + z''^2)}}{2\sqrt{s_2} \sqrt{s_3} (4s_2 s_3 z''^2 + (1 - s_2 - s_3)(s_2 + s_3)(x_3''^2 + z''^2))}. \tag{A.10}
\end{aligned}$$

Changing the integration parameters into polar coordinates,

$$\begin{aligned}
\mathcal{J}_4^3 &= 2 \int^{0 \leq a^2 + b^2 \leq 1} 4da db C \frac{1}{\Gamma(\frac{3}{2})} \frac{1}{\Gamma(\frac{1}{2})} \frac{1}{\Gamma(\frac{1}{2})} \\
&\quad \frac{\sqrt{1 - a^2 - b^2} \pi^{3/2} ((a^2 - b^2)z'' + \sqrt{(a^2 + b^2)((1 - a^2 - b^2)x_3''^2 + z''^2)})}{2(4a^2 b^2 z''^2 + (1 - a^2 - b^2)(a^2 + b^2)(x_3''^2 + z''^2))} \\
&= 2 \int_0^1 4r dr \int_0^{\pi/2} d\theta C \frac{1}{\Gamma(\frac{3}{2})} \frac{1}{\Gamma(\frac{1}{2})} \frac{1}{\Gamma(\frac{1}{2})} \\
&\quad \frac{\pi^{3/2} \sqrt{1 - r^2} (\sqrt{r^2((1 - r^2)x_3''^2 + z''^2)} + r^2 z'' \cos(2\theta))}{2(r^2(1 - r^2)(x_3''^2 + z''^2) + r^4 z''^2 \sin(2\theta)^2)}. \tag{A.11}
\end{aligned}$$

We can finally solve the integral in the order of $\theta \rightarrow r$

$$\mathcal{J}_4^3 = 2C \frac{1}{\Gamma(\frac{3}{2})} \frac{1}{\Gamma(\frac{1}{2})} \frac{1}{\Gamma(\frac{1}{2})} \pi^{5/2} \sqrt{\frac{1}{x_3''^2 + z''^2}}. \tag{A.12}$$

Summing the three terms up,

$$\begin{aligned}
\mathcal{J}_4 &= \mathcal{J}_4^1 + \mathcal{J}_4^2 - \mathcal{J}_4^3 \\
&= \frac{a}{16\pi^3 r_{34}^3} (z_3 z_4)^{\frac{3}{2}} \left(\frac{z''^2 \text{EllipticE}[-\frac{x_3''^2}{z''^2}]}{x_3''^2 + z''^2} - \sqrt{\frac{z''^2}{x_3''^2 + z''^2}} \right) \\
&= \frac{a\lambda}{128\pi^3} (z_3 z_4)^{\frac{3}{2}} (\bar{K}_{xx_3} \bar{K}_{xx_4})^{\frac{3}{2}} \left(\sqrt{1 + \alpha^2} \text{EllipticE}[-\alpha^2] - (1 + \alpha^2) \right), \tag{A.13}
\end{aligned}$$

where the covariant quantity α is defined in (4.4).

B Spectral Function

In this section we recap how to extract dual CFT data from spectral functions of bulk correlator.

B.1 Disconnected Diagrams

The spectral function of the disconnected diagram, given in [23] for AdS_4 and $\Delta = 2$, can be generalized to any spacetime and conformal dimension as

$$D^{(\text{disc})}(\nu) = \frac{\Gamma(\frac{d}{2} - \Delta)^2 \Gamma(\Delta - \frac{d}{4} + i\frac{\nu}{2}) \Gamma(-\frac{d}{4} + \Delta - i\frac{\nu}{2}) \Gamma(\frac{d}{2}) \Gamma(\frac{d}{2} - i\nu) \Gamma(\frac{d}{4} + i\frac{\nu}{2})^2}{2\pi \Gamma(\frac{3d}{4} - \Delta + i\frac{\nu}{2}) \Gamma(\frac{3d}{4} - \Delta - i\frac{\nu}{2}) \Gamma(i\nu) \Gamma(\frac{d}{4} - i\frac{\nu}{2})^2 \Gamma(\Delta)^2}, \quad (\text{B.1})$$

with the unperturbed, 0-th order OPE coefficients given by

$$A_{n,0} = -2\pi i \text{Res} D^{(\text{disc})}(\nu_n). \quad (\text{B.2})$$

B.2 Tree Level Contact interaction

We start with the boundary three point function given by [24]

$$\begin{aligned} W_\nu(x_1, x_2, x_0) &= \int_{\text{AdS}_{d+1}} d^{d+1}y \bar{\Lambda}_\Delta(x_1, y) \bar{\Lambda}_\Delta(x_2, y) \bar{\Lambda}_{\Delta(\nu)}(x_0, y) \\ &= b_{\Delta, \Delta, \nu} \frac{1}{x_{12}^{2\Delta - \Delta(\nu)} x_{10}^{\Delta(\nu)} x_{20}^{\Delta(\nu)}}, \end{aligned} \quad (\text{B.3})$$

$$b_{\Delta, \Delta, \nu} = \frac{1}{2^{4\pi d}} \frac{\Gamma(\Delta - \frac{d}{4} + i\frac{\nu}{2}) \Gamma(\Delta - \frac{d}{4} - i\frac{\nu}{2}) \Gamma(\frac{d}{4} + i\frac{\nu}{2})^2}{\Gamma(\Delta + 1 - \frac{d}{2})^2 \Gamma(1 + i\nu)}, \quad (\text{B.4})$$

out of which we reconstruct the 4-point interaction by insertion of a delta function in the bulk represented as

$$\delta(Y_1 - Y_2) = \int_{\mathbb{R}} d\nu \frac{\nu^2}{\pi} \int_{\text{AdS}_{d+1}} d^d x_0 \bar{\Lambda}_{\Delta(\nu)}(Y_1, x_0) \bar{\Lambda}_{\Delta(-\nu)}(Y_2, x_0) \quad (\text{B.5})$$

as shown in Figure 5. The four point, tree level diagram is then reconstructed as

$$\begin{aligned} W^\times(x_1, x_2, x_3, x_4) &= -\lambda \int_{\mathbb{R}} d\nu \frac{\nu^2}{\pi} \int_{\partial \text{AdS}_{d+1}} d^d x_0 W_\nu(x_1, x_2, x_0) W_{-\nu}(x_0, x_3, x_4) \\ &= -\lambda \int_{\mathbb{R}} d\nu \frac{\nu^2}{\pi} b_{\Delta, \Delta, \nu} b_{\Delta, \Delta, -\nu} \Psi_{x_1, x_2, x_3, x_4, \nu}^{\Delta, \Delta, \Delta, \Delta} \\ &= -\lambda \int_{\mathbb{R}} d\nu \frac{\nu^2}{\pi} b_{\Delta, \Delta, \nu} b_{\Delta, \Delta, -\nu} K(\nu) g_{x_1, x_2, x_3, x_4, \nu}^{\Delta, \Delta, \Delta, \Delta} \\ &:= \int_{\mathbb{R}} d\nu D^\times(\nu) g_{x_1, x_2, x_3, x_4, \nu}^{\Delta, \Delta, \Delta, \Delta}. \end{aligned} \quad (\text{B.6})$$

where we have used (4.12)(4.14),(4.15) and (4.13). Hence we read off

$$D^\times(\nu) = -\lambda \frac{\nu^2}{\pi} b_{\Delta, \Delta, \nu} b_{\Delta, \Delta, -\nu} K(\nu). \quad (\text{B.7})$$

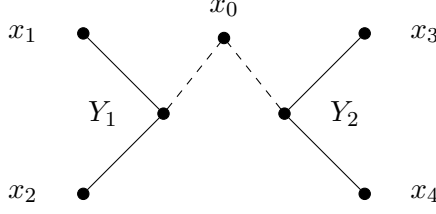


Figure 5. Spectral representation of the cross diagram

The conformal block $g_{x_1, x_2, x_3, x_4, \nu}^{\Delta, \Delta, \Delta, \Delta}$ is regular while $D^{\text{cross}}(\nu)$ has double poles at $\nu_n = \Delta + n - \frac{d}{4}$. Therefore, after closing the contour in the $-\nu$ half plane, residue theorem yields

$$\begin{aligned}
& W^{\times}(x_1, x_2, x_3, x_4) \\
&= -2\pi i \sum_{n=0}^{\infty} \text{Res} (D^{\times}(\nu) g_{x_1, x_2, x_3, x_4, \nu}^{\Delta, \Delta, \Delta, \Delta}, \nu = \nu_n) \\
&= \sum_{n=0}^{\infty} \left(\underbrace{-2\pi i D_{\nu_n}^{\times(-2)} g^{(1)}(x_1, x_2, x_3, x_4, \nu_n)}_{= \gamma_{n,0}^{(1)} A_{n,0} g'_{n,0}} - \underbrace{2\pi i D_{\nu_n}^{\times(-1)} g^{(0)}(x_1, x_2, x_3, x_4, \nu_n)}_{= \gamma_{n,0}^{(1)} A_{n,0}^{(1)} g_{n,0}} \right). \tag{B.8}
\end{aligned}$$

where $f_{\nu_n}^{(i)}$ denotes the i -th order Laurent series coefficient of $f(\nu)$ expanded around $\nu = \nu_n$, and in the last line a comparison is made to the conformal block expansion of the cross diagram,

$$W^{\times}(x_1, x_2, x_3, x_4) = \sum_{n=0}^{\infty} \left(\gamma_{n,0}^{(1)} A_{n,0} g'_{n,0} + \gamma_{n,0}^{(1)} A_{n,0}^{(1)} g_{n,0} \right). \tag{B.9}$$

Plugging (B.2) into (B.8), we conclude that

$$\gamma_{n,0}^{(1)} = \frac{-2\pi i D_{\nu_n}^{\times(-2)}}{A_{n,0}} = \frac{D_{\nu_n}^{\times(-2)}}{\text{Res} D^{\text{(disc)}}(\nu_n)}, \tag{B.10}$$

$$A_{n,0}^{(1)} = \frac{-2\pi i D_{\nu_n}^{\times(-1)}}{\gamma_{n,0}^{(1)}}. \tag{B.11}$$

In the special case of $d = 2$ and $\Delta = \frac{3}{2}$, we have

$$\gamma_{n,0}^{(1)} = \frac{\lambda}{16\pi(n+1)} \tag{B.12}$$

and it is verified that (B.11) agrees with the formula given by [32] that

$$A_{n,0}^{(1)} = \frac{1}{2\gamma_{n,0}^{(1)}} \frac{\partial(A_{n,0} \gamma_{n,0}^{(1)})}{\partial n}, \tag{B.13}$$

in which our conventions are related to [32] by

$$A_{n,l} + \gamma_{n,l}^{(1)} A_{n,l}^{(1)} = (\bar{c}_{n,l} + \delta c_{n,l})^2, \quad A_{n,l} = \bar{c}_{n,l}^2, \quad \gamma_{n,l}^{(1)} A_{n,l}^{(1)} = 2\bar{c}_{n,l} \delta c_{n,l}. \tag{B.14}$$

B.3 One Loop Level

It has been observed in [23, 3.1] that one can make use of the delta function (B.5) to write the one-loop level spectral function for the s -channel as

$$D^{\langle\rangle}(\nu) = D^{\times}(\nu)B(\nu), \quad (\text{B.15})$$

where $B(\nu)$ is the the Källén–Lehmann spectral representation of the intermediate double trace operator that is dual to the bubble diagram (considered a two point function in the $x_1 \rightarrow x_2$ and $x_3 \rightarrow x_4$ limit), as shown in Figure 4.2. The s -channel four-point function at one loop level thus reads

$$\begin{aligned} W^{\langle\rangle}(x_1, x_2, x_3, x_4) &= \int_{\mathbb{R}} \frac{d\nu}{2\pi} D^{\times}(\nu) B(\nu) g_{x_1, x_2, x_3, x_4, \nu}^{\Delta, \Delta, \Delta, \Delta} \\ &= 2\pi i \text{Res} \left(\frac{1}{2\pi} D^{\times}(\nu) B(\nu) g_{x_1, x_2, x_3, x_4, \nu}^{\Delta, \Delta, \Delta, \Delta}, \nu = \nu_n \right). \end{aligned} \quad (\text{B.16})$$

We expect $B(\nu)$ to have simple poles at $\nu_n = \Delta + n - \frac{d}{4}$ ², resulting in the following expansion

$$\begin{aligned} &2\pi i \text{Res} (D^{\times}(\nu) B(\nu) g_{x_1, x_2, x_3, x_4, \nu}^{\Delta, \Delta, \Delta, \Delta}, \nu = \nu_n) \\ &= \underbrace{2\pi i D_{\nu_n}^{\times(-2)} B_{\nu_n}^{(-1)} g^{(2)}(\nu_n)}_{=\frac{1}{2}(\gamma_{n,0}^{(1)})^2 A_{n,0} g_{n,0}''} + \underbrace{2\pi i D_{\nu_n}^{\times(-1)} B_{\nu_n}^{(-1)} g^{(1)}(\nu_n)}_{=(\gamma_{n,0}^{(1)})^2 A_{n,0}^{(1)} g_{n,0}'} + \underbrace{2\pi i D_{\nu_n}^{\times(-2)} B_{\nu_n}^{(0)} g^{(1)}(\nu_n)}_{=\gamma_{n,0}^{(2)} A_{n,0} g_{n,0}'} \\ &+ \underbrace{2\pi i D_{\nu_n}^{\times(0)} B_{\nu_n}^{(-1)} g^{(0)}(\nu_n)}_{=\frac{1}{2}(\gamma_{n,0}^{(1)})^2 A_{n,0}^{(2)} g_{n,0}} + \underbrace{2\pi i D_{\nu_n}^{\times(-2)} B_{\nu_n}^{(1)} g^{(0)}(\nu_n)}_{=(\gamma_{n,0}^{(1)})^2 A_{n,0}^{(1)} g_{n,0}} + \underbrace{2\pi i D_{\nu_n}^{\times(-1)} B_{\nu_n}^{(0)} g^{(0)}(\nu_n)}_{=\gamma_{n,0}^{(2)} A_{n,0}^{(1)} g_{n,0}}, \end{aligned} \quad (\text{B.17})$$

where each term is matched with their counterpart in the conformal block expansion,

$$\begin{aligned} &W^{\langle\rangle}(x_1, x_2, x_3, x_4) \\ &= \sum_{n=0}^{\infty} \left(\frac{1}{2}(\gamma_{n,0}^{(1)})^2 \left(A_{n,0} g_{n,0}'' + 2A_{n,0}^{(1)} g_{n,0}' + A_{n,0}^{(2)} g_{n,0} \right) + \gamma_{n,0}^{(2)} \left(A_{n,0}^{(1)} g_{n,0} + A_{n,0} g_{n,0}' \right) \right). \end{aligned} \quad (\text{B.18})$$

Be aware here that $g^{(2)}(\nu_n) = \frac{1}{2}g_{n,0}''$. Plugging in (B.10) and (B.11), we found that two terms in (B.17) each independently gives a consistent expression of the second order anomalous dimension,

$$\gamma_{n,0}^{(2)} = \frac{2\pi i}{A_{n,0}} D_{\nu_n}^{\times(-2)} B_{\nu_n}^{(0)} = \gamma_{n,0}^{(1)} B_{\nu_n}^{(0)}, \quad (\text{B.19})$$

$$\gamma_{n,0}^{(2)} = \frac{2\pi i}{A_{n,0}^{(1)}} D_{\nu_n}^{\times(-1)} B_{\nu_n}^{(0)} = \gamma_{n,0}^{(1)} B_{\nu_n}^{(0)}. \quad (\text{B.20})$$

Similarly, the second order OPE coefficient is found to be

$$A_{n,0}^{(2)} = \frac{2\pi i}{(\gamma_{n,0}^{(1)})^2} (D_{\nu_n}^{\times(0)} B_{\nu_n}^{(-1)} + D_{\nu_n}^{\times(-2)} B_{\nu_n}^{(1)})_{\nu_n}. \quad (\text{B.21})$$

²This is verified by (4.19).

The first term in (B.17) provides also a consistency check that

$$B_{\nu_n}^{(-1)} = \frac{1}{D_{\nu_n}^{\times(-2)}} (\gamma_{n,0}^{(1)})^2 A_{n,0} = \gamma_{n,0}^{(1)}, \quad (\text{B.22})$$

giving rise to a constraint on $B_{\nu_n}^{(-1)}$,

$$B_{\nu_n}^{(-1)} = \frac{(-1)^n \pi^{2-\frac{3d}{2}} \lambda \Gamma\left(\frac{d}{2} + n\right) \Gamma(d - n - 2\Delta) \Gamma(\Delta)^2 \Gamma(n + \Delta)^2 \Gamma\left(-\frac{d}{2} + n + 2\Delta\right) \Gamma\left(\frac{d-2n-2\Delta}{2}\right)^2}{16n! \Gamma\left(\frac{d}{2}\right) \Gamma\left(\frac{d}{2} - \Delta\right)^2 \Gamma\left(1 - \frac{d}{2} + \Delta\right)^4 \Gamma(2n + 2\Delta) \Gamma(d - 2n - 2\Delta)}. \quad (\text{B.23})$$

Up to normalization, this is in fact the same argument as [5, 4.24], that $B_{\nu_n}^{(-1)}$ must have residues at $\frac{d}{2} + i\nu = 2\Delta + 2n$ which cancels precisely with the contribution from the generalized free field theory. It is one of the constraints that allowed for the bootstrap of an explicit expression of B_{ν_n} . The first few OPE coefficients squared at $\mathcal{O}(\lambda)$ are given in Table 5.

	$\Omega_{n,0}$
$n = 0$	$\frac{5}{2} - 4 \log 2$
$n = 1$	$\frac{69}{64} - \frac{9}{4} \log 2$
$n = 2$	$\frac{1755}{8192} - \frac{4050}{8192} \log 2$
$n = 3$	$\frac{48335}{1572864} - \frac{117600}{1572864} \log 2$
$n = 4$	$\frac{15789375}{4294967296} - \frac{39690000}{4294967296} \log 2$
$n = 5$	$\frac{336159}{85899345920} - \frac{865125}{85899345920} \log 2$
$n = 6$	$\frac{13520857669}{351843720888320} - \frac{17656192720}{351843720888320} \log 2$

Table 5. First few squared OPE coefficients at $\mathcal{O}(\lambda)$

C Conformal Block

The conformal block with an intermediate operator dimension $\tilde{\Delta} = 2\Delta + 2n + l$ is given in [33] by

$$G_{\tilde{\Delta}(n,l),l} = \sum_{k=0}^{\infty} u^{\frac{\tilde{\Delta}-l}{2}+k} \sum_{m=0}^{2k} A_{k,m} f_{k,m}(1-v), \quad (\text{C.1})$$

with

$$\begin{aligned} f_{k,m}(1-v) &= (1-v)^{l-m} {}_2F_1\left(\frac{\tilde{\Delta}+l}{2} + k - m - a, \frac{\tilde{\Delta}+l}{2} + k - m + b, \tilde{\Delta} + l + 2k - 2m; 1-v\right) \\ &= \sum_{p=0}^{\infty} \frac{\left(\frac{\tilde{\Delta}+l}{2} + k - m - a\right)_p^2}{p! \left(\tilde{\Delta} + l + 2k - 2m\right)_p} (1-v)^{l-m+p}, \end{aligned} \quad (\text{C.2})$$

and

$$\begin{aligned}
A_{k,m}(\tilde{\Delta}) = & \sum_{m_1, m_2=0}^{\lfloor \frac{m}{2} \rfloor} \frac{1}{2^{l-1}} (-1)^{m+m_1+1} 4^{m_1+m_2} \frac{(-l)_m (-\lfloor m/2 \rfloor)_{m_1+m_2} (k - \lfloor m/2 \rfloor) + 1/2)_{m_1}}{m! m_1! m_2! (k - m + m_1)!} \\
& \times \frac{(\tilde{\Delta} - 1)_{2k-m} (d/2 - \tilde{\Delta})_{m-k-m_1-m_2} (l - \tilde{\Delta} + d - 1)_{2(\lfloor m/2 \rfloor - m_2) - m}}{(\tilde{\Delta} + l - m - 1)_{2k-m} (\tilde{\Delta} + l)_{2(k+m_1 - \lfloor m/2 \rfloor) - m}} \\
& \times \frac{(1 - d/2 - l - k + m - m_1 + m_2) (3/2 - d/2 - \ell + \lfloor (m+1)/2 \rfloor)_{m_2}}{(2 - d/2 - l)_{-k+m+m_2} (-1 + d/2 + l - m_2)_{k-m+m_1+m_2+1}} \\
& \times \prod_{\alpha \in \{\pm a, \pm b\}} \left(\left(\frac{1}{2} (\tilde{\Delta} + l) + \alpha \right)_{k-m+m_1} \left(\frac{1}{2} (\tilde{\Delta} - l - d + 2) + \alpha \right)_{m_2} \right) (1 + (4ab-1)(m \bmod 2)),
\end{aligned} \tag{C.3}$$

where $a = \frac{\Delta_1 - \Delta_2}{2}$ and $b = \frac{\Delta_3 - \Delta_4}{2}$. $(x)_n := \frac{\Gamma(x+n)}{\Gamma(x)}$ is the Pochhammer symbol.

The squared OPE coefficients are given in [32] by

$$A_{[\mathcal{O}_i \mathcal{O}_j]_n, l}^{i,j} = \frac{2^l (-1)^l (\Delta_i - \frac{d}{2} + 1)_n (\Delta_j - \frac{d}{2} + 1)_n (\Delta_i)_{l+n} (\Delta_j)_{l+n}}{l! n! (l + \frac{d}{2})_n (\Delta_i + \Delta_j + n - d + 1)_n (\Delta_i + \Delta_j + 2n + l - 1)_l (\Delta_i + \Delta_j + n + l - \frac{d}{2})_n}, \tag{C.4}$$

Given the conformal block, it is also possible to determine the OPE coefficients from (2.14) and (2.15), yielding the same result as above. Note that $\frac{1}{2^{l-1}}$ and 2^l were added to (C.3) and (C.4) so that our normalization matches that in [25].

For arbitrary n and l , the condition for $G_{n,l}$ to contribute a $u^i(1-v)^j$ is that

$$\frac{\tilde{\Delta} - l}{2} = \frac{2\Delta + 2n + l - l}{2} \leq \Delta + i, \tag{C.5}$$

so that $n \leq i$ and $k = i - n$. In addition,

$$l - m \leq l - 2k \leq l - 2i + 2n \leq j. \tag{C.6}$$

In the conformal block expansion (2.18), contribution to the $u^i(1-v)^j$ term is therefore

$$\sum_{n=0}^i \sum_{l=0, l \text{ even}}^{2i+j-2n} \mathcal{A}_{n,l} \mathcal{G}_{n,l}. \tag{C.7}$$

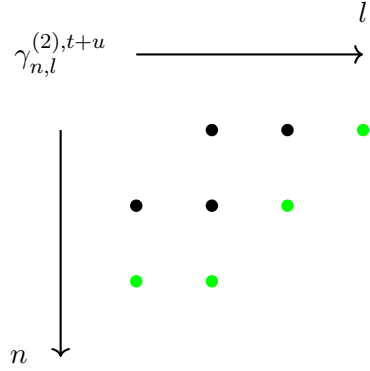


Figure 6. Recursive relations

D Recursive Relation

Any $\gamma_{n,l}^{(2),t+u}$ can be computed with a recursive relation and 5 initial values. The initial values are

$$\gamma_{n,l}^{(2),t+u} = \begin{cases} -\frac{\lambda^2}{96\pi^2}, & (n,l) = (0,0), \\ -\frac{\lambda^2}{3360\pi^2}, & (n,l) = (0,1), \\ -\frac{\lambda^2}{15840\pi^2}, & (n,l) = (0,2), \\ -\frac{13\lambda^2}{3360\pi^2}, & (n,l) = (1,0), \\ -\frac{61\lambda^2}{221760\pi^2}, & (n,l) = (1,1). \end{cases} \quad (\text{D.1})$$

For any $n \geq 1$ and $l \geq 2$, $\gamma_{n,l}^{(2),t+u}$, $\gamma_{n-1,l}^{(2),t+u}$, $\gamma_{n-1,l+2}^{(2),t+u}$ (marked in Figure 6 as green dots) can be expressed as polynomials of $\gamma_{n+1,l-2}^{(2),t+u}$, $\gamma_{n+1,l}^{(2),t+u}$, $\gamma_{n,l+2}^{(2),t+u}$, $\gamma_{n-1,l+4}^{(2),t+u}$ (marked as black dots), together with n and l . The explicit expressions of these polynomials are given in (D.2)-(D.5).

When $n \geq 2$ and $l = 0$,

$$\begin{aligned} \gamma_{n,l}^{(2),t+u} = & \left(-(1+l+n)(55 + 8l^3 + 126n + 64n^2 + 4l^2(13 + 6n) + 2l(51 + 60n + 8n^2)) \gamma_{n-2,l/2+1}^{(2),t+u} \right. \\ & + (35 + 24l + 4l^2)(3 + l + n)(5 + 2l + 2n) \gamma_{n-2,l/2+2}^{(2),t+u} \\ & - (2 + l + n)(15 + 8l^3 + l^2(36 - 8n) - 114n - 64n^2 - 2l(-23 + 36n + 8n^2)) \gamma_{n-1,l/2+1}^{(2),t+u} \\ & + (8l^4 + 4l^3(9 + 8n) + 2l^2(23 + 54n + 20n^2) + n(15 + 46n + 32n^2) \\ & \left. + l(15 + 92n + 104n^2 + 16n^3)) \gamma_{n-1,l/2}^{(2),t+u} \right) \\ & \times \left(8(1+n)(1+l+n)(5+2l^2+4n+l(7+2n)) \right)^{-1}. \end{aligned} \quad (\text{D.2})$$

when $n \geq 1$ and $l \geq 4$.

$$\begin{aligned}
\gamma_{n,l}^{(2),t+u} = & \left(-2n(166 + 16l^5 + 13n - 632n^2 + 548n^3 - 128n^4 + 16l^4(-8 + 5n) \right. \\
& + 8l^3(41 - 72n + 18n^2) + 8l^2(-31 + 159n - 112n^2 + 14n^3) \\
& + l(-131 - 888n + 1492n^2 - 576n^3 + 32n^4) \right) \gamma_{n-1,l-2}^{(2),t+u} \\
& + 2n(16l^5 + 16l^4(-2 + 5n) + 8l^3(-7 - 24n + 18n^2) \\
& + n(-3 + 64n + 36n^2 - 64n^3) + 8l^2(9 - 9n - 44n^2 + 14n^3) \\
& + l(-3 + 136n + 20n^2 - 256n^3 + 32n^4) \right) \gamma_{n-1,l/2}^{(2),t+u} \\
& + (525 - 220l - 1401l^2 + 1792l^3 - 872l^4 + 192l^5 - 16l^6 \\
& + 665n - 4621ln + 6292l^2n - 3480l^3n + 864l^4n - 80l^5n \\
& - 2800n^2 + 6120ln^2 - 4460l^2n^2 + 1344l^3n^2 - 144l^4n^2 \\
& + 1680n^3 - 2132ln^3 + 864l^2n^3 - 112l^3n^3 \\
& \left. - 280n^4 + 192ln^4 - 32l^2n^4 \right) \gamma_{n,l-4}^{(2),t+u} \\
& + (-30 + 92l + 18l^2 - 320l^3 + 400l^4 - 192l^5 + 32l^6 \\
& + 36n + 468ln - 1816l^2n + 2240l^3n - 1120l^4n + 192l^5n \\
& + 394n^2 - 2496ln^2 + 4104l^2n^2 - 2432l^3n^2 + 448l^4n^2 \\
& - 1032n^3 + 3152ln^3 - 2528l^2n^3 + 512l^3n^3 \\
& + 888n^4 - 1280ln^4 + 288l^2n^4 - 256n^5 + 64ln^5) \gamma_{n,l-2}^{(2),t+u} \Big) \\
& \times \left(15 + 16l^6 + 113n + 112l^5n + 250n^2 + 120n^3 - 160n^4 - 128n^5 \right. \\
& + 8l^4(-11 - 8n + 38n^2) + 8l^3(-8 - 59n - 40n^2 + 50n^3) \\
& + l^2(57 - 132n - 868n^2 - 576n^3 + 256n^4) \\
& \left. + l(64 + 263n + 40n^2 - 644n^3 - 448n^4 + 64n^5) \right)^{-1}. \tag{D.3}
\end{aligned}$$

When $n = 0$ and $l \geq 6$,

$$\begin{aligned}
\gamma_{n,l}^{(2),t+u} = & \left(-(-12339 + 128l^9 - 8361n + 176934n^2 \right. \\
& + 25280n^3 - 111672n^4 + 108656n^5 - 51456n^6 + 8192n^7 \\
& + 64l^8(-27 + 20n) + 32l^7(241 - 558n + 152n^2) + 144l^6(-35 + 644n - 460n^2 + 64n^3) \\
& + 8l^5(-7313 - 23706n + 43708n^2 - 14760n^3 + 1168n^4) \\
& + 4l^4(42747 - 520n - 204336n^2 + 149568n^3 - 27360n^4 + 1216n^5) \\
& + 2l^3(-77493 + 265566n + 343520n^2 - 665136n^3 + 261856n^4 - 25344n^5 + 512n^6) \\
& + l(42282 + 253365n - 423578n^2 - 292884n^3 + 657736n^4 - 352896n^5 + 60160n^6) \gamma_{n,l-4}^{(2),t+u} \\
& + 2(-387 + 128l^9 + 72n + 19417n^2 - 17754n^3 - 26204n^4 + 34584n^5 - 9728n^6) \\
& + 64l^8(-19 + 18n) + 32l^7(121 - 348n + 128n^2) + 16l^6(-251 + 2366n - 2456n^2 + 464n^3) \\
& + 8l^5(-401 - 6312n + 17076n^2 - 8608n^3 + 912n^4) \\
& + 4l^4(2467 - 402n - 52444n^2 + 58088n^3 - 15984n^4 + 928n^5) \\
& + 2l^3(-3021 + 36196n + 53480n^2 - 179056n^3 + 99904n^4 - 15040n^5 + 384n^6) \\
& + 2l(825 + 10472n - 39751n^2 - 13724n^3 + 80620n^4 - 47184n^5 + 6432n^6) \gamma_{n,l-2}^{(2),t+u} \\
& + (2+n) \left((99 - 40l + 4l^2)(-84 + 32l^6 + 45n + 1002n^2 - 540n^3 + 72n^4 \right. \\
& + 16l^5(-19 + 12n) + 16l^4(59 - 95n + 28n^2) + 8l^3(-125 + 480n - 342n^2 + 64n^3) \\
& + l^2(98 - 3496n + 4920n^2 - 2128n^3 + 288n^4) \\
& + l(269 + 1212n - 3036n^2 + 2096n^3 - 608n^4 + 64n^5) \gamma_{n+1,l-6}^{(2),t+u} \\
& - (-990 + 128l^8 + 1203n + 30790n^2 - 32260n^3 - 8808n^4 + 16768n^5 - 4096n^6 \\
& + 192l^7(-9 + 4n) + 32l^6(273 - 310n + 56n^2) + 16l^5(-1335 + 2908n - 1340n^2 + 128n^3) \\
& + 8l^4(3231 - 13574n + 10500n^2 - 2760n^3 + 144n^4) \\
& + 4l^3(-3009 + 35180n - 40240n^2 + 14608n^3 - 2720n^4 + 64n^5) \\
& - 2l^2(1525 + 50346n - 90744n^2 + 33392n^3 - 1600n^4 + 1024n^5) \\
& + l(4371 + 30636n - 119764n^2 + 58032n^3 + 23712n^4 - 13120n^5) \gamma_{n+1,l-4}^{(2),t+u} \left. \right) \\
& \times \left((3 - 8l + 4l^2)(1 + l + n)(1 + 2l + 2n) \right. \\
& \times (-57 + 16l^5 - 166n + 384n^2 + 480n^3 - 256n^4 + 16l^4(-5 + 6n) \\
& + 8l^3(-1 - 62n + 26n^2) + 8l^2(31 + 28n - 132n^2 + 24n^3) \\
& + l(1 + 748n + 732n^2 - 896n^3 + 64n^4)) \left. \right)^{-1}. \tag{D.4}
\end{aligned}$$

When $n \geq 2$ and $l = 2$,

$$\begin{aligned}
\gamma_{n,l}^{(2),t+u} = & \left((3 + 8l + 4l^2)(-5 + 8l^4 - 7n - 2n^2 + 4l^3(3 + 8n) \right. \\
& + l^2(-6 + 20n + 40n^2) + l(-15 - 20n + 8n^2 + 16n^3)) \gamma_{n-2,l/2+1}^{(2),t+u} \\
& + (-39 - 32l^6 + l^5(16 - 192n) + 89n + 46n^2 - 224n^3 + 128n^4 \\
& + l^4(224 + 80n - 544n^2) - 8l^3(45 - 112n - 40n^2 + 112n^3) \\
& - 2l^2(-51 + 540n - 584n^2 - 320n^3 + 384n^4) \\
& + l(89 + 204n - 944n^2 + 544n^3 + 384n^4 - 256n^5)) \gamma_{n-2,l/2}^{(2),t+u} \\
& + (-18 + 69l - 14l^2 - 232l^3 + 336l^4 - 176l^5 + 32l^6 \\
& + 21n + 76ln - 576l^2n + 944l^3n - 592l^4n + 128l^5n \\
& - 6n^2 - 152ln^2 + 560l^2n^2 - 544l^3n^2 + 160l^4n^2 \\
& + 48ln^3 - 128l^2n^3 + 64l^3n^3) \gamma_{n-1,l-2}^{(2),t+u} \\
& + (-9l + 30l^2 + 8l^3 - 112l^4 + 112l^5 - 32l^6 \\
& - 9n + 36ln - 144l^2n - 656l^3n + 720l^4n \\
& + 6n^2 - 312ln^2 - 1264l^2n^2 + 1376l^3n^2 + 608l^4n^2 \\
& - 160n^3 - 976ln^3 + 1024l^2n^3 + 1600l^3n^3 \\
& - 256n^4 + 256ln^4 + 1536l^2n^4 + 512ln^5) \gamma_{n-1,l/2}^{(2),t+u} \\
& \times \left(8(1+n)(1+l+n)(-3 + 8l^4 - 16n - 16n^2 + 4l^3(3 + 10n) \right. \\
& \left. + l^2(-6 + 32n + 64n^2) + l(-11 - 26n + 16n^2 + 32n^3)) \right)^{-1}.
\end{aligned} \tag{D.5}$$

References

- [1] I. Heemskerk, J. Penedones, J. Polchinski and J. Sully, *Holography from Conformal Field Theory*, *JHEP* **10** (2009) 079 [[arXiv:0907.0151](https://arxiv.org/abs/0907.0151)].
- [2] E. Witten, *Anti-de Sitter space and holography*, *Adv. Theor. Math. Phys.* **2** (1998) 253 [[hep-th/9802150](https://arxiv.org/abs/hep-th/9802150)].
- [3] I. Bertan and I. Sachs, *Loops in Anti-de Sitter Space*, *Phys. Rev. Lett.* **121** (2018) 101601 [[arXiv:1804.01880](https://arxiv.org/abs/1804.01880)].
- [4] I. Bertan, I. Sachs and E.D. Skvortsov, *Quantum ϕ^4 Theory in AdS_4 and its CFT Dual*, *JHEP* **02** (2019) 099 [[arXiv:1810.00907](https://arxiv.org/abs/1810.00907)].
- [5] D. Carmi, L. Di Pietro and S. Komatsu, *A Study of Quantum Field Theories in AdS at Finite Coupling*, *JHEP* **01** (2019) 200 [[1810.04185](https://arxiv.org/abs/1810.04185)].
- [6] D. Carmi, *Loops in AdS : From the Spectral Representation to Position Space*, *JHEP* **06** (2020) 049 [[1910.14340](https://arxiv.org/abs/1910.14340)].
- [7] S.L. Cacciatori, H. Epstein and U. Moschella, *Loops in anti de Sitter space*, *JHEP* **08** (2024) 109 [[2403.13142](https://arxiv.org/abs/2403.13142)].

- [8] T. Heckelbacher, I. Sachs, E. Skvortsov and P. Vanhove, *Analytical evaluation of AdS_4 Witten diagrams as flat space multi-loop Feynman integrals*, [2201.09626](#).
- [9] T. Heckelbacher and I. Sachs, *Loops in dS/CFT* , *JHEP* **02** (2021) 151 [[2009.06511](#)].
- [10] C. Sleight and M. Taronna, *Bootstrapping Inflationary Correlators in Mellin Space*, *JHEP* **02** (2020) 098 [[1907.01143](#)].
- [11] C. Sleight and M. Taronna, *From dS to AdS and back*, *JHEP* **12** (2021) 074 [[2109.02725](#)].
- [12] L. Di Pietro, V. Gorbenko and S. Komatsu, *Analyticity and Unitarity for Cosmological Correlators*, [2108.01695](#).
- [13] T. Heckelbacher, I. Sachs, E. Skvortsov and P. Vanhove, *Analytical evaluation of cosmological correlation functions*, *JHEP* **08** (2022) 139 [[2204.07217](#)].
- [14] C. Chowdhury, A. Lipstein, J. Mei, I. Sachs and P. Vanhove, *The subtle simplicity of cosmological correlators*, *JHEP* **03** (2025) 007 [[2312.13803](#)].
- [15] M. Nowinski and I. Sachs, *Resummation of Cosmological Correlators and their UV-Regularization*, [2507.21224](#).
- [16] L. Dolan, C.R. Nappi and E. Witten, *Conformal operators for partially massless states*, *JHEP* **10** (2001) 016 [[hep-th/0109096](#)].
- [17] O. Aharony, S.S. Gubser, J.M. Maldacena, H. Ooguri and Y. Oz, *Large N field theories, string theory and gravity*, *Phys. Rept.* **323** (2000) 183 [[hep-th/9905111](#)].
- [18] J.M. Maldacena, *The large N limit of superconformal field theories and supergravity*, *Adv. Theor. Math. Phys.* **2** (1998) 231 [[hep-th/9711200](#)].
- [19] I.R. Klebanov and E. Witten, *AdS / CFT correspondence and symmetry breaking*, *Nucl. Phys. B* **556** (1999) 89 [[hep-th/9905104](#)].
- [20] F.A. Dolan and H. Osborn, *Conformal four point functions and the operator product expansion*, *Nucl. Phys. B* **599** (2001) 459 [[hep-th/0011040](#)].
- [21] O.W. Greenberg, *Generalized Free Fields and Models of Local Field Theory*, *Annals Phys.* **16** (1961) 158.
- [22] F.A. Dolan and H. Osborn, *Implications of $N=1$ superconformal symmetry for chiral fields*, *Nucl. Phys. B* **593** (2001) 599 [[hep-th/0006098](#)].
- [23] I. Sachs and P. Vanhove, *Bulk Landau pole and unitarity of dual conformal field theory*, *JHEP* **07** (2023) 106 [[2303.03491](#)].
- [24] D. Meltzer, E. Perlmutter and A. Sivaramakrishnan, *Unitarity Methods in AdS/CFT* , *JHEP* **03** (2020) 061 [[1912.09521](#)].
- [25] T. Heckelbacher, *On holographic methods in cosmology*, Ph.D. thesis, Munich U., 2022. 10.5282/edoc.30174.
- [26] C. Schneider, “RISCERgoSum.” <https://www3.risc.jku.at/research/combinat/software/ergosum/>, 2026.
- [27] M. Kauers, “Guess.” <https://risc.jku.at/sw/guess/>, 2026.
- [28] B. Basso and G.P. Korchemsky, *Anomalous dimensions of high-spin operators beyond the leading order*, *Nucl. Phys. B* **775** (2007) 1 [[hep-th/0612247](#)].

- [29] L.F. Alday, A. Bissi and T. Lukowski, *Large spin systematics in CFT*, *JHEP* **11** (2015) 101 [[arXiv:1502.07707](https://arxiv.org/abs/1502.07707)].
- [30] L.F. Alday and A. Zhiboedov, *An Algebraic Approach to the Analytic Bootstrap*, *JHEP* **04** (2017) 157 [[arXiv:1510.08091](https://arxiv.org/abs/1510.08091)].
- [31] A. Bissi, A. Sinha and X. Zhou, *Selected topics in analytic conformal bootstrap: A guided journey*, *Phys. Rept.* **991** (2022) 1 [[2202.08475](https://arxiv.org/abs/2202.08475)].
- [32] A.L. Fitzpatrick and J. Kaplan, *Unitarity and the Holographic S-Matrix*, *JHEP* **10** (2012) 032 [[arXiv:1112.4845](https://arxiv.org/abs/1112.4845)].
- [33] W. Li, *Lightcone expansions of conformal blocks in closed form*, *JHEP* **06** (2020) 105 [[1912.01168](https://arxiv.org/abs/1912.01168)].